CHARACTERISTICS OF COHERENT STRUCTURES IN MARINE ATMOSPHERIC SURFACE LAYER

Hua Shuai

Thesis submitted to the Faculty of the
Virginia Polytechnic Institute and State University
in partial fulfillment of the requirements for the degree of

MASTER of SCIENCE
in
OCEAN ENGINEERING

Dr. Wayne L. Neu, Chair
Dr. Roger L. Simpson
Dr. Stergios Liapis

July 22, 1997
Blacksburg, Virginia

Keywords: Coherent structure, Marine atmosphere, Boundary layer

CHARACTERISTICS OF COHERENT STRUCTURES IN MARINE ATMOSPHERIC SURFACE LAYER

Hua Shuai

(ABSTRACT)

Wind speed data of multi-heights have been examined to investigate the spatial and temporal characteristics of coherent structures in the near neutral marine atmospheric surface layer. With Taylor's hypothesis, the temporal velocity signals have been transformed to spatial fluctuations and then visualize these spatial velocity fluctuations to identify the coherent structures. It has been confirmed that there exist similar coherent structures in the marine atmospheric surface layer to those in laboratory turbulent boundary layer. These similar coherent structures include ejections, sweeps, shear layers, transverse vortices, and combined events of the shear layers and transverse vortices. Besides these similar coherent structures, there exist the plume and downdraft motions in the unstable marine atmospheric surface layer.

It has been observed that the streamwise spatial length of the ejections and sweeps is 20–250 m and their mean frequency is of order of 10^{-2}–10^{-3} s^{-1} at mean wind speed of 5–12.6 m/s. Between the region of the upstream ejection and downstream sweep motions an inclined shear layer is often seen. The inclined angle of the shear layer has been observed to vary from 30° to 70° with the height and length of the the shear layer. The transverse vortices are seen to exist in every region from the wall up to a height of 45 m and their

diameter is up to 40 m. The mean frequency of the shear layers and the transverse vortices is of order of 10^{-3} s^{-1}. In the fully developed stage of the combined event of the shear layer and transverse vortex, the shear layer is generally longer and the diameter of the transverse vortex is larger. The mean frequency of the combined event of the shear layers and the transverse vortices is of order of 10^{-3} s^{-1}. The streamwise spatial length of the plume and downdraft motions is generally from 20 m to 50 m.

Analysis indicates that the mean wind speed is a dominant factor in affecting the spatial and temporal characteristics of the coherent structures in the near neutral marine atmospheric surface layer. As the mean wind speed increases, the frequency of the shear related coherent events will increase, while the frequency of the buoyancy related coherent events (plumes and downdrafts) will decrease. The temperature difference between higher level of the surface layer and sea surface is the second main factor in affecting the spatial and temporal characteristics of the coherent structures. As the marine atmospheric surface layer becomes more stable the coherent motions will be suppressed. The effect of the temperature difference on the buoyancy related plume and downdraft motions is more evident than on the other shear related coherent motions.

Dedicate to my father and mother, my wife and my family

ACKNOWLEDGMENTS

I would like to express my deepest appreciation to Dr. Wayne L. Neu, my advisor and mentor, for all of his advice, support and encouragement during the completion of my graduate program and this thesis.

I would like to thank Dr. Roger L. Simpson and Dr. Stergios Liapis for their comments on this thesis and serving in my committee.

I would also like to thank Dr. Ravi S. Boppe for all his help and discussing a lot of my questions.

I would like to acknowledge my parents for their constant support and encouragement throughout my educational pursuit.

I would especially like to thank my wife, Meng Bao, for all her support and patience while I pursue this degree.

NOMENCLATURE

x	Streamwise coordinate
y	Transverse coordinate
z	Wall-normal coordinate
u	Streamwise velocity component
v	Transverse velocity component
w	Wall-normal velocity component
u'	Fluctuation component in streamwise velocity
v'	Fluctuation component in transverse velocity
w'	Fluctuation component in wall-normal velocity
U_m	Mean wind speed across the measuring heights
ρ	Air density
ν	Kinematic viscosity
τ_0	Shear stress at surface of the wall
δ	Boundary layer thickness
U_∞	Mean velocity in the free stream
u_*	Friction velocity $= \sqrt{\tau_0/\rho} = \sqrt{-\overline{u'w'}}$
z^+	zu_*/ν
T	Temperature

dT47–10	Temperature difference between a height of 47 m and 10 m above sea surface
Q_1	The first quadrant events (x-z plane), or outward interaction events
Q_2	The second quadrant events (x-z plane), or ejection events
Q_3	The third quadrant events (x-z plane), or inward interaction events
Q_4	The fourth quadrant events (x-z plane), or sweep events
SL	Shear layer events
TV	Transverse vortex events
CS	Combination structure events of shear layer and transverse vortex
P	Plume events
D	Downdraft events
Ni	Number of the same type of events in same streamwise length
Nt	Total number of the same type of events
Ne	Number of the same type of events in each data file

Contents

List of Figures

List of Tables

Chapter 1

INTRODUCTION

Turbulent flow structures in the boundary layer have been studied by many fluid dynamicists for several decades in an attempt to understand the dynamics of the turbulent flow. Extensive literature in this field has been published. Among these works, one of the most important discoveries is that of coherent motions in turbulent boundary layer flow. It is this discovery that spurred studying of turbulent boundary layer flow into a new stage.

1.1 Background

1.1.1 Coherent Motions in the Laboratory Turbulent Boundary Layer

Organized flow structures in laboratory turbulent boundary layer over a flat plate were identified by Kline *et al.* (1967) with a flow visualization technique. They observed that low speed streaks were formed in the region very near the wall ($z^+ \leq 10$). These streaky

motions distributing at rather large spanwise spacing gradually lift up downstream, waver and oscillate, then suddenly leap away from the wall and outward to the outer region ($z^+ \geq 40$) where they break up violently and interact with the outer flow. They further conjectured that the ejections of the low speed fluid away from the wall and then breakup in the outer region were responsible for the energy, momentum and vorticity transfer between the inner and outer layer. Corino and Brodkey (1969) also concluded that the ejection was the most important feature in the wall region for turbulent pipe flow. These ejections were the major contributors to the production of turbulence and were independent of mean flow parameters. They further estimated that 70% of Reynolds stress was a result of ejection at about a Reynolds number of 20,000. In examining the relation between bursting and the production of turbulence for a flat plate flow, Kim *et al.* (1971) found that essentially all the production of turbulence in the zone $0 \leq z^+ \leq 100$ occured during bursting times. They divided the bursting process into three stages from the lifting of the low speed streaks away from the innermost layer to the breakup of the well-defined motion into more chaotic motion associated by a return to the wall of the low speed streaks.

We must distinguish the bursting event from the ejection event. Although it is always associated with the ejection of fluid away from the wall, a bursting event is defined as an overall process from the lifting to the breakup of low speed streak filaments. A bursting event may involve only one or several ejection events grouped together. Moreover, the individual ejection events occur more often than the bursting events.

Because the flow visualization techniques are limited to qualitative observation in low Reynolds number (of order of 10^4–10^5 based on boundary layer thickness) turbulent flow, since 1971, conditional-sampling techniques have been developed for more detailed studying on the flow structures in turbulent boundary layer. The conditional-sampling techniques can be used to study high Reynolds number flow and also give more quantitative information of flow velocity features. With the conditional-sampling techniques many more

detailed characteristics of the coherent structures in turbulent boundary layer have been studied. Using short time autocorrelation of streamwise component of velocity signal Kim *et al.* (1971) found that the first positive peak in the autocorrelation had a lag time which well corresponded with the value of average time between bursts obtained from flow visualization. Lu and Willmarth (1973) introducing a quadrant technique found that the ejections ($u' < 0,\ w' > 0$) were the largest contributor to Reynolds shear stress $-\rho\overline{u'w'}$ (77% of the total stress) and sweeps ($u' > 0,\ w' < 0$) the second largest (55% of the total stress). Two additional types of motion, outward interaction ($u' > 0,\ w' > 0$) and inward interaction ($u' < 0,\ w' < 0$), gave rise to negative Reynolds stress and accounted for the surplus stress (over 100% of the net value) produced by ejection and sweep events. Blackwelder and Kaplan (1976) identified the existence of the coherent motions in turbulent boundary layer with a variable-interval time averaging (VITA) technique which detects the large variances in streamwise velocity signal. These large variances are thought to be the signatures of the individual ejection and sweep events.

Each of the detection techniques is based on a unique velocity signal pattern which is assumed to be a characteristic associated with a event and can be detected by a specified detection function. However, the different conditional-sampling methods could get different results for the same velocity probe data because of the different criteria used in these methods. Bogard and Tiederman (1986) evaluated the effectiveness of the different conditional-sampling methods by making direct comparisons with flow visualization. They concluded that the quadrant technique had a high probability of detecting the ejection events with higher reliability.

1.1.2 Categories and Models of the Coherent Structures in Laboratory Turbulent Boundary Layer

Although organized motions in turbulent boundary layer have been repeatedly identified, there is no universal classification of these organized motions. The fundamental complexity of turbulence phenomena and the different detection techniques created a wide variety of coherent motions and different interpretations of their role in turbulence production. In an attempt to construct a combined and universal conceptual model of the coherent structures with the state of knowledge, Robinson (1991) reviewed many known coherent structures in low Reynolds number canonical turbulent boundary layer flow and classified eight categories of coherent motions as follows.

1. Low speed streaks in the near wall region

Low speed streaks consist of narrow streaks of the slow moving fluid which may be created by vortices. Low speed means that the fluctuation component in streamwise velocity is below zero ($u' < 0$).

2. Ejections

As the low speed streaks move downstream they rise gradually away from the wall and then violently erupt outward from the wall in a short period of time which are called ejection events. These lifted low speed streaks, which may create new vortices, eventually break up in the outer region as a last stage of the so called "bursting" event which originates from the formation of the low speed streaks. The ejection events can be recognized with a signature of negative fluctuation components in streamwise velocity ($u' < 0$) as well as positive fluctuation components in wall-normal velocity ($w' > 0$).

3. Sweeps

It is called a sweep event that high speed fluid rushes in from the outer region toward the wall at a small angle of incidence. The sweep events can be recognized with a signature of positive fluctuation components in streamwise velocity ($u' > 0$) as well as negative fluctuation components in wall-normal velocity ($w' < 0$).

4. Vortical structures

Although a wide variety of vortical structures has been proposed, the quasi-stream-wise vortex and inclined horseshoe-shaped vortex or hairpin-shaped vortex in higher Reynolds number flow are commonly accepted vortical structures as shown in Figure 1.1. They are thought to be the essential coherent structures for turbulence production cycle. It is very difficult to characterize the spatial geometry shape of these three-dimensional vortical structures with the flow visualization techniques and single-point velocity measurement data. Only with multi-point velocity signal data could the spatial characteristics of these structures be analyzed.

5. Near wall shear layer

In the near wall zone, between the narrow streaks of high and low speed fluid regions, the shear rates ($\frac{\partial u}{\partial y}$, $\frac{\partial u}{\partial z}$) are greater than the local mean values and small shear layer vortices could be formed.

6. Near wall pockets

In the sublayer or lower log layer there are some pocket-like regions from which the marked fluid in the flow is drawn away. These pockets may be created by the vortical motions.

7. Large scale motions in the outer region

Large transverse vortical structures are commonly observed to be associated with large scale three-dimensional bulges in the turbulent/potential interface. Through the large scale bulges the irrotational fluid is entrained into the turbulent region and the vorticity of turbulent region may be transferred into the potential region.

8. Shear layer "backs" of large scale motions

A inclined shear layer interface near the upstream side of the large scale motions is often called the "back" of large scale motions as shown in Figure 1.2. This shear layer interface is also a sharp interface of the streamwise velocity between high and low speed fluid region and often extends from the wall to the outer region. While the shear layer "back" of large scale motions associates the large transverse vortices, some new transverse vortices may be created by rollup of the shear layer back just as shown in Figure 1.3 which means that the outer region may be more active in the production of turbulence.

The eight categories of coherent structures are the basic elements of the conceptual model of the structures in the canonical turbulent boundary layer and have been widely accepted now. Based on these categories of the coherent motions, a combined conceptual model was built. Among the eight elements of the coherent motions which one is the principal element to the continuity of turbulence production is still under controversy. With direct numerical simulation of turbulent boundary layer, the vortical structures are found to be associated with each of the other coherent motions. In other words, each class of the coherent motions could have a relationship with the vortical structures in certain dynamic ways as shown in Figure 1.1. It is hypothesized that the vortical motions give rise to the other events and hence are the central events which are responsible for the production of turbulence throughout the boundary layer, although it is confusing to try to distinguish cause from

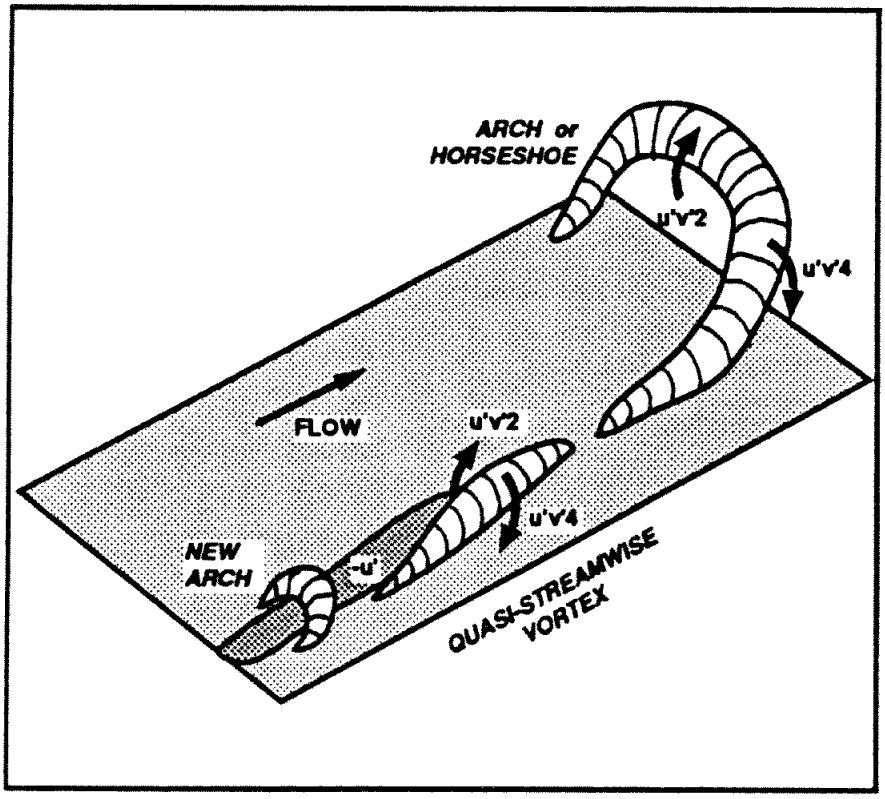

Figure 1.1: Vortical structures and production of Reynolds stress in a low Re flat plate boundary layer (from Robinson, 1990).

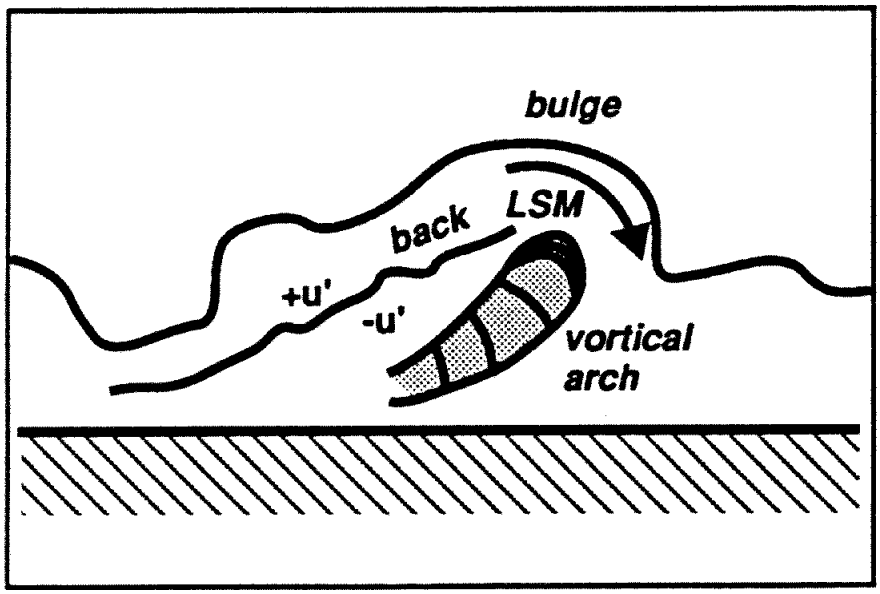

Figure 1.2: The shear layer "back" of the large scale motion (LSM) associated with a vortical arch (from Robinson, 1990).

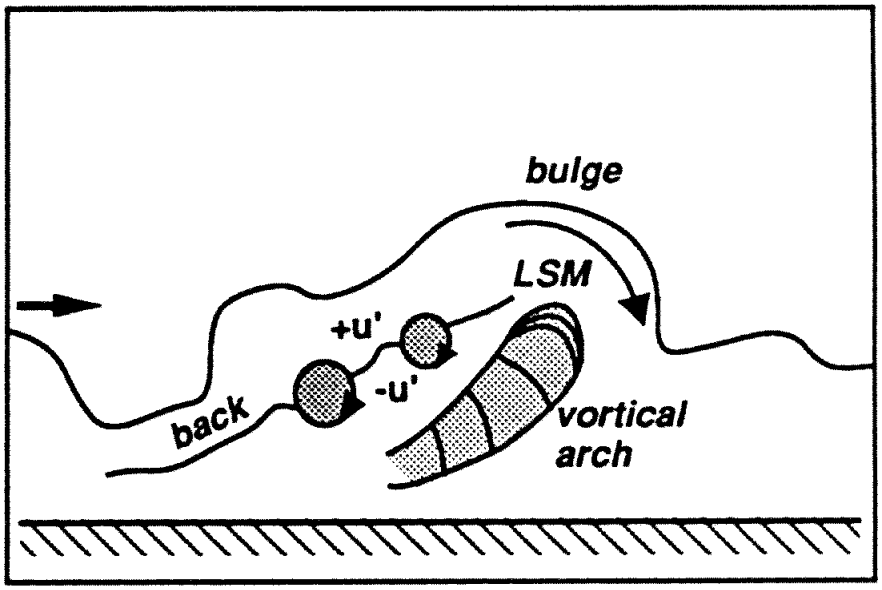

Figure 1.3: Transvers vortices may be created by rollup of the shear layer "back" of the large scale motion (LSM) associated with a vortical arch (from Robinson, 1990).

effect of the coherent motions since the other events can also create new vortical motions.

Some features of the combined structure model may be universal, although it is built in low Reynolds number canonical turbulent boundary layer. Therefore, some structures of this combined model may be extended to atmospheric boundary surface layer.

1.1.3 Coherent Motions in the High Reynolds Number Turbulent Boundary Layer

Because of the limitation of direct measurement techniques, it is difficult to get experimental data for high Reynolds number turbulent boundary layer flow in laboratory. There are not as many works on high Reynolds number turbulent flow structures as on low Reynolds number turbulent flow. But the organized motions such as ejection and sweeping phenomena in high Reynolds number turbulent flow have also been observed with the conditional-sampling techniques. These coherent motions may be universal features of turbulent flow, at both high and low Reynolds numbers.

In investigating the bottom turbulent structures of an estuarine tidal flow Gordon (1974) found that turbulent momentum transport was intermittent. Heathershaw (1974) also reported the bursting phenomena and the intermittence of turbulence and Reynolds stress generation in the bottom boundary layer of the sea tidal currents. With simultaneous temperature traces at several heights in the first eight meters in the atmospheric surface layer Phong-anant *et al.* (1980) observed that an organized structure existed in near wall region. This organized motion was associated with a gradual rise in temperature followed by a sharp decrease in temperature downstream (ramplike feature). They suggested that the organized motion was similar to a three dimensional horseshoe vortex inclined to the wall. Boppe (1995) using the conditional-sampling techniques in the velocity probe data

of sea wind identified the existence of the ejection and sweeping structures in the marine atmospheric surface layer. He concluded that the organized structures extended across the depth of the surface layer and inclined at an angle while convecting downstream. Högström and Bergström (1996) also identified the coherent structures with Tiederman's (1988) detection method in the atmospheric surface layer wind data from three fields with very different surface roughness characteristics. They found that 90% of momentum transport was carried out by the bursts, or ejections, and sweeps. They further suggested that the bursts, or ejections, and sweeps associated with the large arch or horseshoe-shaped vortical structures.

1.2 Objectives of the Present Work

There is no doubt for the existence of coherent structures in both low and high Reynolds number flow in the turbulent boundary layer, but their dynamics and natures remain largely unsettled. The need for better understanding the dynamics of the atmospheric surface turbulent flow requires that its flow structures be studied in more detail. The study of the flow structure in the marine atmospheric surface layer is of great important to understand the momentum, heat and moisture transfer between air and sea. An understanding of air-sea fluxes is necessary for the predication of weather and ocean currents. The intermittent quasi-periodic nature of the coherent structures in the marine atmospheric surface layer may be in large part responsible for intermittency of air properties over the ocean. Radar is refracted and scattered as it passes through varying air masses which are caused by the intermittency of air properties. The influences on radar propagation may be inferred by understanding the coherent structures in the marine atmospheric surface layer. Furthermore, the study of the characteristics of the coherent structures will greatly help in building turbulence models and turbulence numerical simulations. Inspired by earlier

research work, especially by the work done by Boppe and Neu (1995), the present study tries to make more quantitative study on these coherent structures.

The major difference between the atmospheric boundary layer and engineering scale boundary layer is at the outer edge. The thickness of the marine atmospheric boundary layer is defined by a capping inversion or an inversion layer, the height of which above the sea surface depends on the profile of virtual potential temperature instead of $0.99U_\infty$ as in the flat plate boundary layer, where U_∞ is the mean velocity in the free stream. The inversion layer at the top of the marine atmospheric boundary layer acts as a lid to the rising thermals and restrains the domain of turbulence within the marine atmospheric boundary layer. Above the capping inversion there is the free atmosphere where no turbulence exists. The thickness of the atmospheric boundary layer is quite variable in time and space, ranging from hundreds of meters to a few kilometers. The presence of the ocean wave is the other feature of the marine atmospheric boundary layer. However, the wave height is much less than the scale of the thickness of the marine atmospheric boundary layer. So the wave effects are not to be considered in the present work.

The main object of the present thesis is to present a general picture about coherent structures in the marine atmospheric surface turbulent flow based on multi-point wind data. Experimental data collected from a measuring tower standing in the sea have been studied in the present work. The experimental data include vector wind speed and direction fluctuations at different heights from 3 m to 45 m above the sea surface. For high Reynolds number marine atmospheric surface turbulent flow there are some coherent structures which are similar to those of engineering turbulent flow and some special features as well. These structures consist of ejections, sweeps, vortices, shear layers, combination structures of shear layers and transverse vortices, plumes and downdrafts. The marine atmospheric boundary layer may extend up to 1000 m or more in height, depending on atmospheric stability, so the region up to 45 m above the sea surface is still in the atmospheric surface

layer region (the lowest 10 % of the atmospheric boundary layer is defined as surface layer).

This thesis attempts to analyze the spatial and temporal characteristics of turbulent flow structures, in the marine atmospheric surface layer up to 45 m height above the sea surface, in order to examine the intermittency of the air-sea fluxes. The experiment site and data will be briefly described in chapter 2. Chapter 3 describes the spatial and temporal characteristics of the coherent structures which have been seen in the present study with the experiment wind data. The effects of wind speeds and air-sea temperature differences on the coherent structures will be analyzed in Chapter 4. Finally, some discussions and conclusions will be given in chapter 5.

Chapter 2

EXPERIMENTAL DATA

2.1 Experiment Site

The data of the Risø Air-Sea Experiments (RASEX) (Barthelmie *et al.* , 1994) have been used in the present study. The wind data at different heights from 3 m to 45 m above the sea surface and temperature data were recorded during the experiments. The measurements were conducted at an offshore wind farm at Vindeby in Denmark during the spring and fall of 1994. The experiment site is situated off the northwestern coast of the island of Lolland and the water depth here is between 2.1 m and 5.1 m. Eleven wind turbines (marked by 1W–5W, 1E–6E) were arranged in two rows oriented along an axis of 325–145° (clockwise from north). Figures 2.1 and 2.2 show the locations of the site and the wind turbines. The most southerly turbine in the array is approximately 1.5 km from land and the turbine spacing is 300 m both along and between the rows.

The data used in the present work were taken from the data recorded with the instruments on one of the three meteorological masts, the sea mast west (SMW) marked by its location.

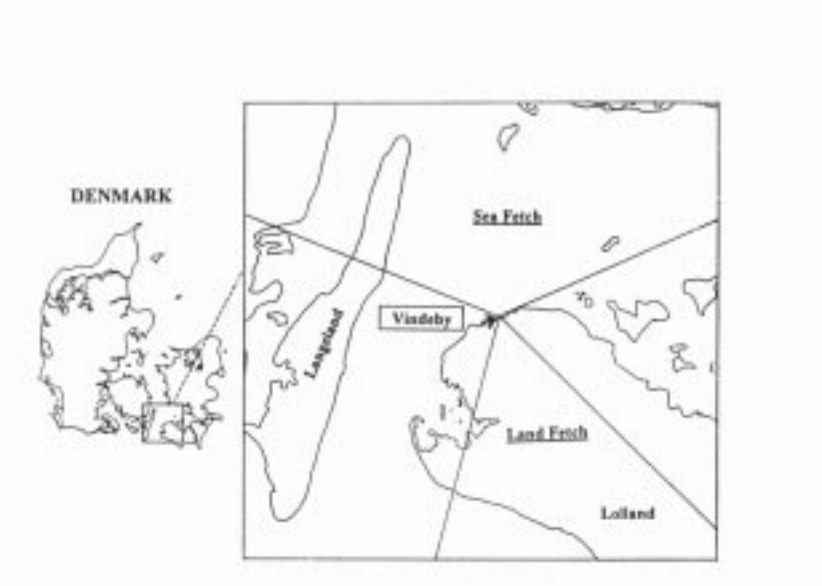

Figure 2.1: Location of Vindeby, Denmark (from Barthelmie *et al.* , 1994).

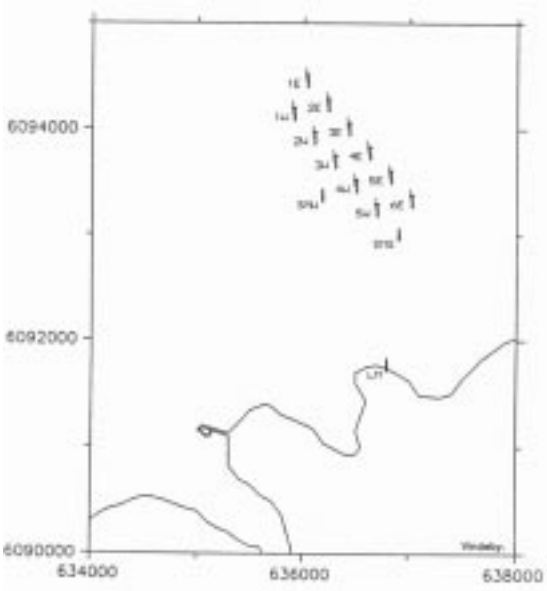

Figure 2.2: The configuration of the wind farm and the positions of the masts at Vindeby (from Barthelmie *et al.* , 1994).

The sea mast west (SMW) had been erected off the shore and to the west at distance of 300 m from the first row of the wind turbines. The land mast (LM) is located nearly 2 km south of the most southerly turbine in the array and the sea mast south (SMS) is located at distance of 300 m south from the first row of the wind turbines. The relative locations of the masts to the wind turbines are shown in Figure 2.2. The minimum distances from land to the sea mast west (SMW) and sea mast south (SMS) are approximately 1630 m and 1270 m respectively.

The topography at Vindeby is very flat and lies close to the sea level. So no topographic enhancement of the wind speed is expected. To the south of the land mast the terrain is mainly open farmland with a few scattered houses and trees and to the north is open sea. The coastline runs approximately along the line of 285–105° (clockwise from north). The distance of the open sea fetch around the land mast is about 15–60 km and that of land fetch is about 11–48 km.

2.2 Experimental Instrumentation

Instruments had been installed at the same heights (with reference to sea surface) on all three 45 m high masts to measure wind speed at three levels, wind direction at two levels, temperature differences and absolute temperature. On the sea mast west (SMW) three cup anemometers (type of Risø PT2244b) and six 3D fast response sonic anemometers (type of F2360a GILL 3 Axis Ultrasonic anemometers) were installed additionally to get more detailed wind profiles. The installation heights of six sonic anemometers were 3, 6, 10, 18, 32 and 45 meter above sea surface respectively. The 3D sonic anemometers, whose wind speed measuring range is from 0 to 60 m/s, can measure vector wind speed/direction fluctuations along with temperature fluctuations.

For measuring temperature at water surface a downward looking IR thermometer was installed on the sea mast west (SMW). Moreover, additional instruments were provided to the SMW to measure water temperatures at different depth, wave heights (with an ultrasonic height sensor) and current speeds and directions (with an electromagnetic current meter) at sea surface.

Data from the sea masts were acquired simultaneously with the PCs equipped in the turbines and transmitted to the land mast (LM) via a underwater fibre optic cable. All the signals were collected and stored on disk at the land mast (LM) to ensure synchronization. Samples were taken at the rate of 20 Hz and stored as half-hourly means together with selected higher resolution time-series.

For more details about the experiments, refer to Barthelmie *et al.* (1994).

2.3 Data Reduction

The instantaneous wind speed amplitude, direction (clockwise from north) and elevation angle are calculated based on the data recorded by the 3D sonic anemometers. For each 30 minute record a mean wind vector $\overline{U}$ is obtained by averaging the instantaneous wind vectors over the entire record. Then the instantaneous wind vectors are transformed to a coordinate system defined by the mean wind vector so that the instantaneous wind vectors can be expressed as $U = (u, v, w)$, where the direction of u is along the direction of the mean wind vector $\overline{U}$, v in the horizontal transverse flow direction and w in the vertical direction for a right hand system. The three components of each instantaneous wind vector can be separated respectively into a mean and a fluctuating part as follows:

$$u = \overline{u} + u' ;$$

$$v = \overline{v} + v' ;$$

$$w = \overline{w} + w'.$$

High-pass filtering has been applied to the velocity fluctuation components in order to filter out very low frequency velocity fluctuation components. These very low frequency velocity fluctuation components are caused by much larger scale flow features, such as local gusts and boundary layer rolls, which will lead to temporarily increase or decrease the streamwise velocity relative to the long time mean value of streamwise velocity. The interest of the present work is only in the local convective motions or local average events rather than the long time average events. Hence for easier detecting the coherent motions, these very low frequency fluctuations have been filtered out by a high-pass filtering. This high-pass filtering for the velocity fluctuations has been achieved by subtracting from each point a 1-minute moving average which is centered at that point and this has caused little distortions of the high frequency fluctuations.

Chapter 3

COHERENT STRUCTURE CHARACTERISTICS

3.1 Transformation of the Data

In order to investigate the spatial structure of the coherent motions in the marine atmospheric surface layer, some data files from the Risø Air-Sea Experiments (RASEX) have been chosen to be examined. Each data file has a half hour time historical record of wind vector. Before each data file was examined the temporal velocity fluctuation components had been transformed to spatial velocity fluctuation components which were relative to a reference frame moving at a speed of U_m, where U_m is the mean wind velocity across the measuring depth in the streamwise direction. This transformation is based on Taylor's hypothesis that temporal measurements at a point can be transformed to spatial patterns with the transformation $x = U_m t$. It is assumed in this transformation that the entire turbulent flow field is frozen in time and then it is horizontally transported past the probe

at a speed of U_m. Although the turbulent flow field in the marine atmospheric surface layer is never really frozen, the duration of the coherent structures is long enough in comparison with the time that they take to pass the probe. Therefore this transformation can well be applied to examine the spatial structure of the coherent motions in the marine atmospheric surface layer. However, it should be noted that an important factor in detecting the coherent motions is that the coherent motions will pass the probe at different stages of their lives as well as at different spanwise distance from their respective center.

3.2 Coherent Structures in the Marine Atmospheric Surface Layer

Following the spatial velocity fluctuations, typical coherent motions can be distinguished very clearly, though the discrimination of the coherent motions is somewhat subjective and the coherent structures are not always typical and easy to be distinguished. The typical coherent structures are shown in Figures 3.1 to 3.10. In these figures, the horizontal coordinate x or t represents a spatial length of 0–150 m or a time value which starts from the origin of the data file, and the vertical coordinate z, whose range is 0–50 m, represents the height from the wall. The spatial velocity fluctuations ($u'w'$) are drawn with blue, red, yellow and green colors, each color respectively represents that the spatial velocity fluctuations are in the first, second, third and fourth quadrant (Q_1, Q_2, Q_3 and Q_4) of the u'-w' plane.

As shown in Figure 3.1, a typical ejection event occurs in the region from x = 20–90 m in which $u' < 0,\ w' > 0$. The length of this ejection region is 70 m and its height is above 45 m. The ejection events often extend beyond the maximum measuring height in the present data. As shown in Figure 3.2, a typical sweep event is seen in the region from

x = 0–150 m in which $u' > 0,\ w' < 0$. The total length of this sweep region is 170 m and its height is above 45 m. Strong sweeps often create small transverse vortices in the near wall region. The ejections and sweeps are not always seen to follow each other in the streamwise direction. There are quite a few individual ejection and sweep events in the marine atmospheric surface layer.

When the upstream sweep motions follow the downstream ejection motions in the streamwise direction, then an inclined shear layer is formed between the regions of these two motions. A typical shear layer structure is as shown in Figure 3.3. The region of the inclined shear layer starts from x $\approx$ 45 m at lower level and ends at x $\approx$ 80 m at higher level. It extends from the wall up to a height of 45 m. The shear layer is formed between the upstream sweep motions and the downstream ejection motions. When the ejections and sweeps are strong, some large shear layer vortices on the shear layer can be observed as shown in Figure 3.4. These shear layer vortices may be caused by the rollup of the shear layer. In the present data it is difficult to find a typical shear layer without the shear layer vortices.

Of the coherent motions in the marine atmospheric surface layer, the most often seen is transverse vortices. It is also difficult to trace these transverse vortices because of their three dimensional spatial characteristics. The limitation of the sensors in one plane (x–z plane) and larger space between the sensors in vertical direction (the vertical space is 3–14 m) also makes it more difficult to trace streamwise vortices and small transverse vortices. A typical transverse vortex is as shown in Figure 3.5. The diameter of this vortex is about 40 m and its center locates at x $\approx$ 100 m, z $\approx$ 20 m. The large scale strong transverse vortices often induce the ejections and sweeps in the upstream and downstream regions, or upward and wallward rotating sides, of the transverse vortices. The transverse vortices exist from the wall region to the region of 45 m height. Hence these transverse vortices may be the most important elements of the turbulence production and momentum transport in

the marine atmospheric surface layer.

A combination structure of the shear layer and the transverse vortex, or the shear layer "back" of the large scale motions as suggested by Robinson (1990), has also been observed in the present data files. As shown in Figure 3.6, the sweep motions ($+u'$ region), which start from x = 0, are upstream of the ejection motions ($-u'$ region), which start from x $\approx$ 30 m at lower level. Between these two regions a sloping shear layer is formed which extends from the wall up to a height of 32 m. The ejection motions are caused by a large downstream transverse vortex whose center located at x $\approx$ 110 m, z $\approx$ 32 m, and its diameter is about 25 m. However, as shown in Figures 3.7 and 3.8, the spatial region of the combination structures is generally larger than that of the combination structure seen in Figure 3.6. In Figure 3.7, the sweep motions, which start from x = 0, are upstream of the ejection motions, which start from x $\approx$ 40 m at lower level. An inclined shear layer is formed between the sweep and ejection motions. It starts from x $\approx$ 40 m at the wall and extends to a point of x $\approx$ 116 m, z = 45 m. Because the streamwise spatial length of the shear layer and large transverse vortex overpasses 150 m, the coordinate frame in Figure 3.7 has to be shifted 70 m downstream in streamwise direction in order to view the downstream large scale transverse vortex which causes the ejections as well as sweeps behind it as shown in Figure 3.8. The upstream shear layer follows the large transverse vortex whose center is located at x $\approx$ 125 m, z $\approx$ 35 m and diameter is about 30 m as shown in Figure 3.8. The large transverse vortex may be the "head" of a large vortical arch and can cause the ejection and sweep motions. This combination event of the shear layer and large transverse vortex may be seen more in the overall marine atmospheric surface layer. Since a lot of the shear layer structures seen in the present data extends beyond the maximum measuring height and they may be larger shear layer "back" of the much larger scale transverse vortex whose "head" is located in a region beyond the maximum measuring height and hence can not be seen by the probe. Besides, the transverse vortex may not always cause the strong

shear layer and the small transverse vortex may cause small shear layer just near the wall region which may well be the initial stage of the combination event of the shear layer and the transverse vortex. So there may exist more of this type of coherent structures in the marine atmospheric surface layer and the combination event of the shear layer and the large scale transverse vortex may well be universal in turbulent boundary layer flow.

When the stability of the marine atmospheric surface layer is unstable, in which the air temperature at higher level is lower than that at sea surface level, the plume and downdraft motions can be seen as shown in Figures 3.9 and 3.10. In Figure 3.9, the region of the plume starts from x $\approx$ 60 m and ends at x $\approx$ 90 m. It extends from the wall up to a height of 45 m. In Figure 3.10, the downdraft motion region starts from x = 30 m and ends at x = 140 m. The flow is downward from a height of 45 m all the way down to the wall. These two types of the coherent motions which are caused by the variations of the air density mainly depend on the stability of the marine atmospheric surface layer, which is related to the the temperature difference between air and sea as well as wind speed. In general, the lower the wind speed and the larger the air temperature difference between the higher and lower levels are, the more the plume and downdraft motions. The relationship between the spatial and temporal characteristics of the coherent structures and the ambient conditions, the mean wind speed and air temperature difference, will be discussed in following sections.

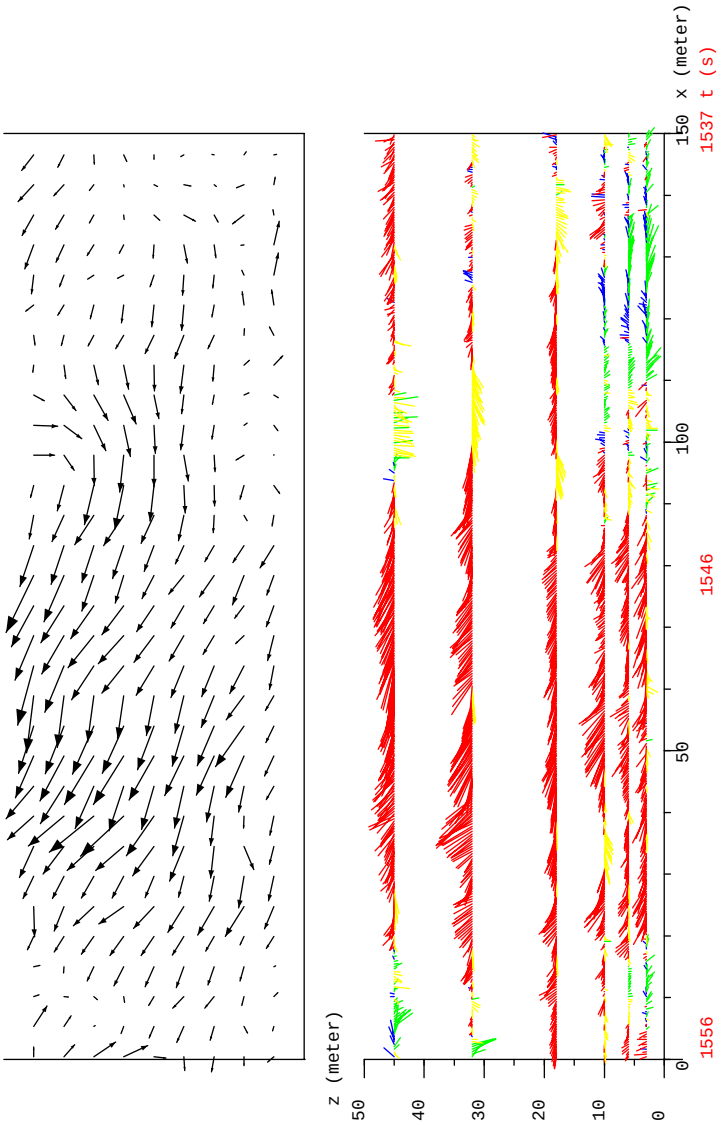

,

Figure 3.1: Ejection Event, spatial velocity fluctuations. The horizontal axis represents the streamwise spatial length x (black number, meter) or the time value t (red number, second) which starts from the origin of the data file. The vertical axis z represents the height above the sea level (meter).

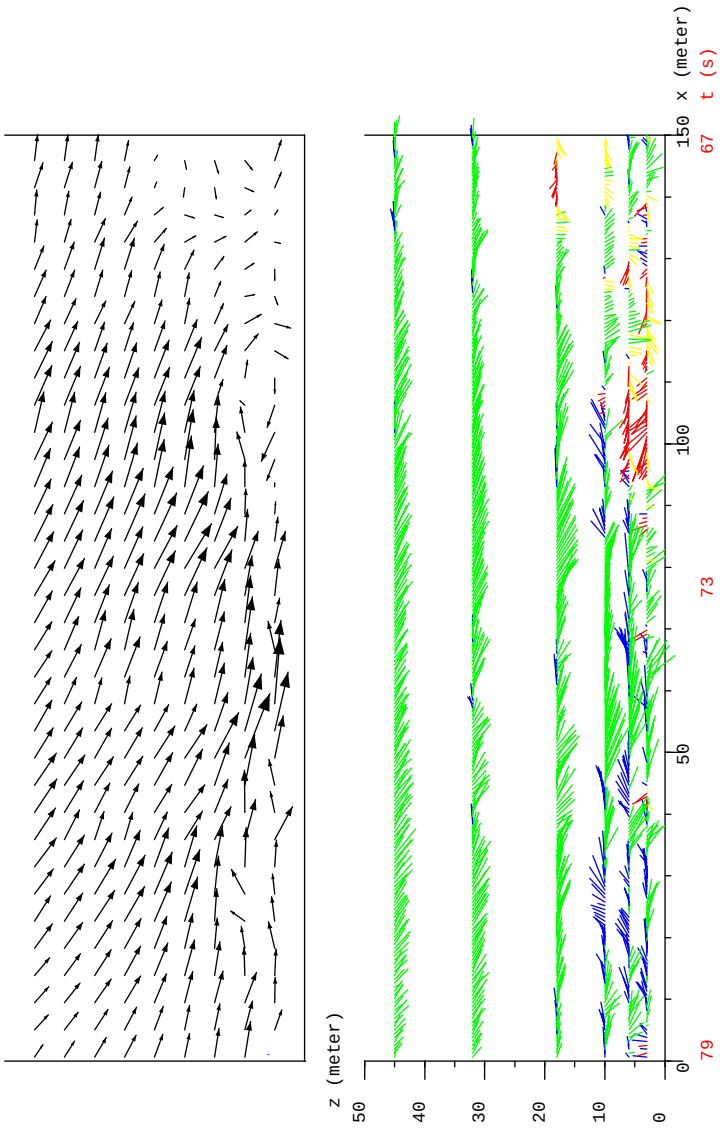

Figure 3.2: Sweep Event.

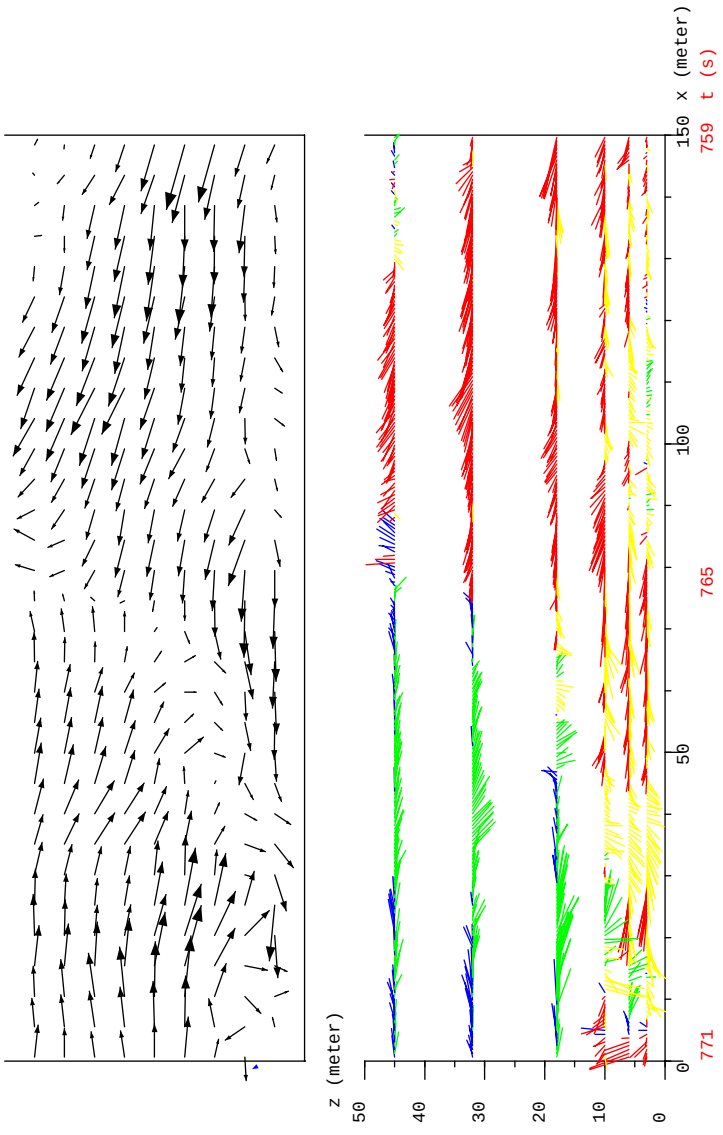

Figure 3.3: Shear Layer Structure.

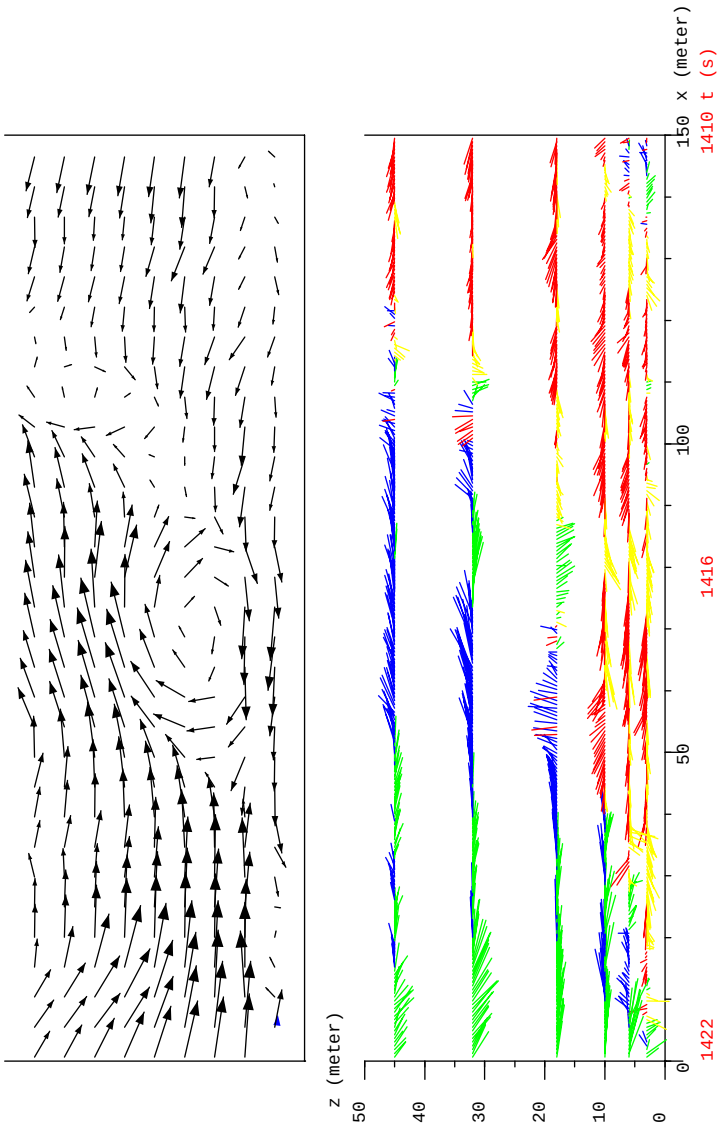

Figure 3.4: Shear Layer with Shear Layer Vortices.

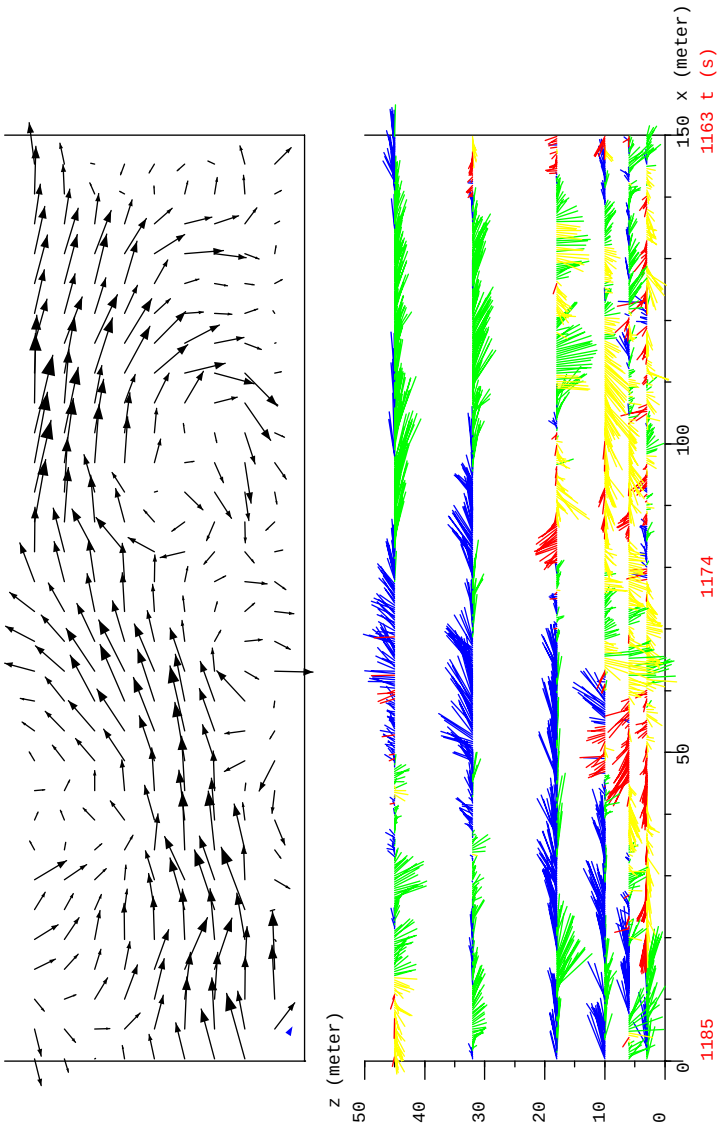

Figure 3.5: Transverse Vortex.

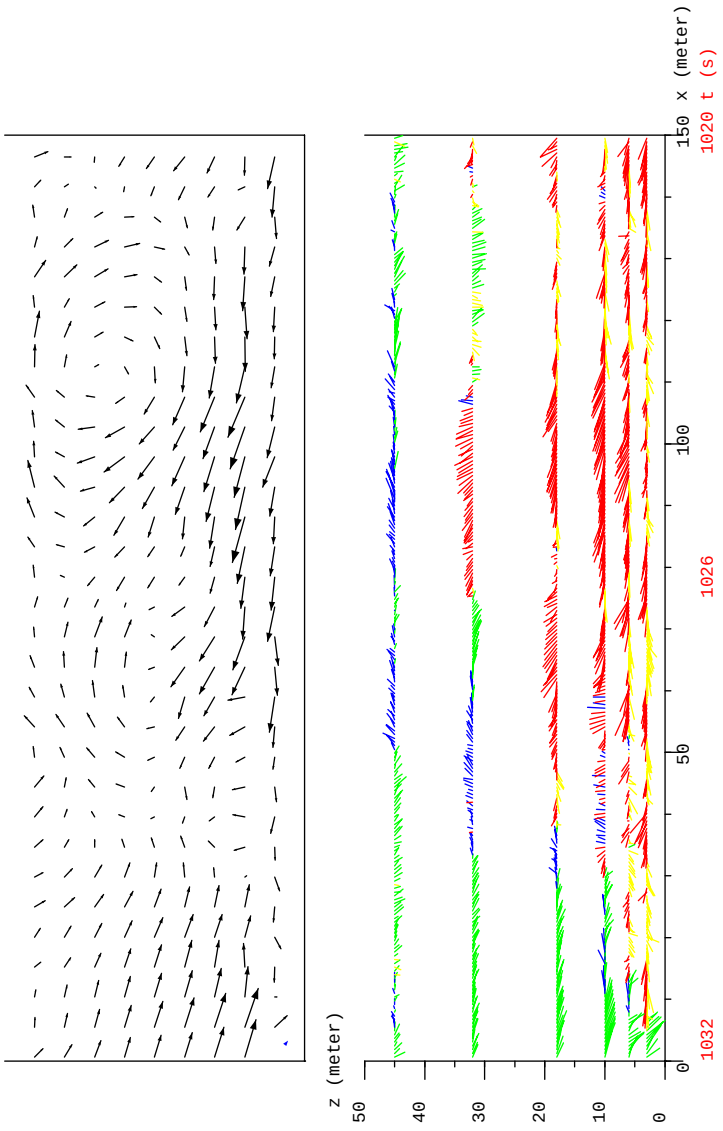

Figure 3.6: Combination Structure of the Shear Layer and Large Transverse Vortex.

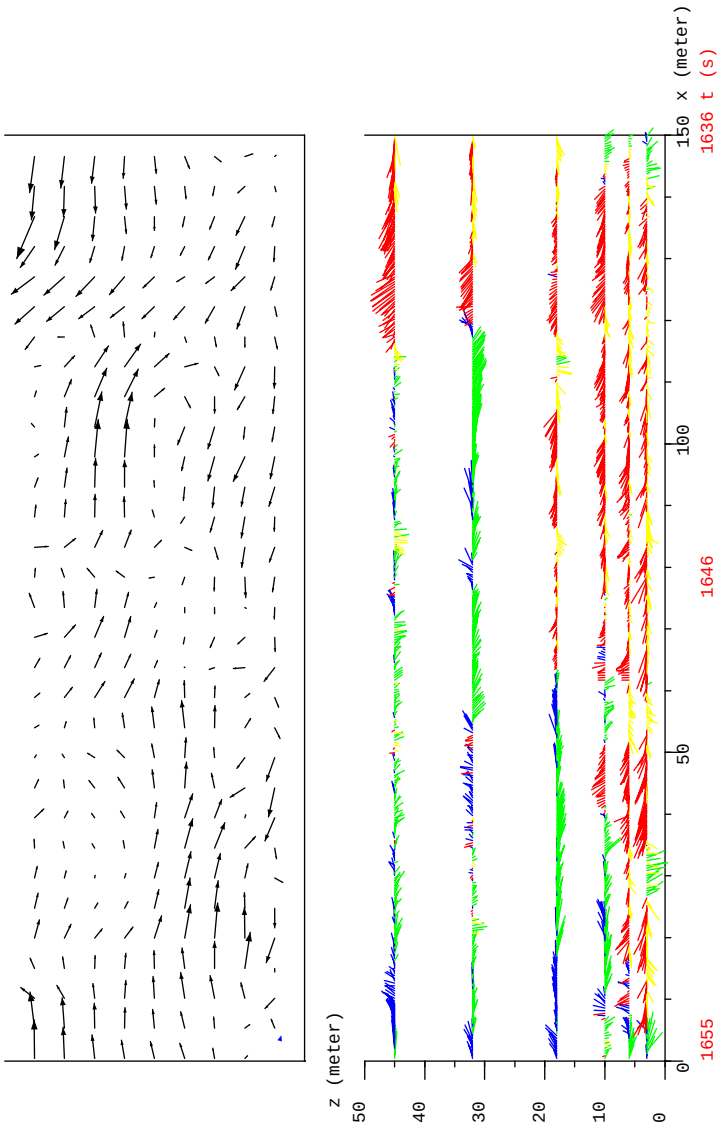

Figure 3.7: Longer Combination Structure of the Shear Layer and Large Transverse Vortex.

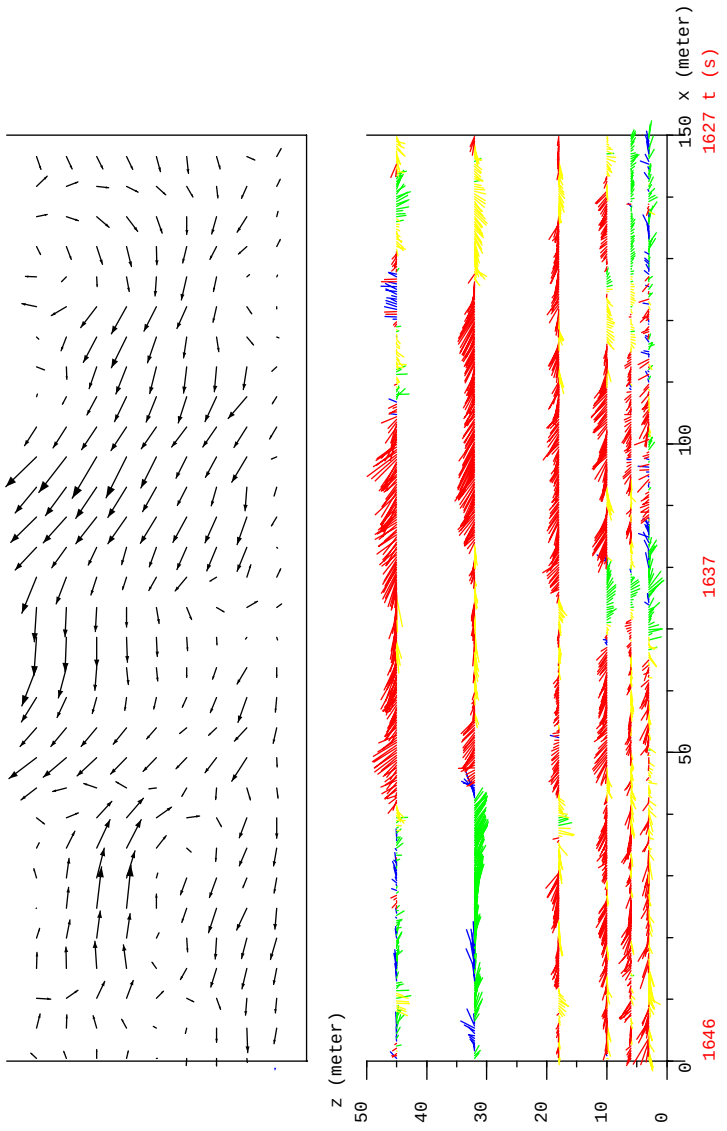

Figure 3.8: Longer Combination Structure of the Shear Layer and Large Transverse Vortex.

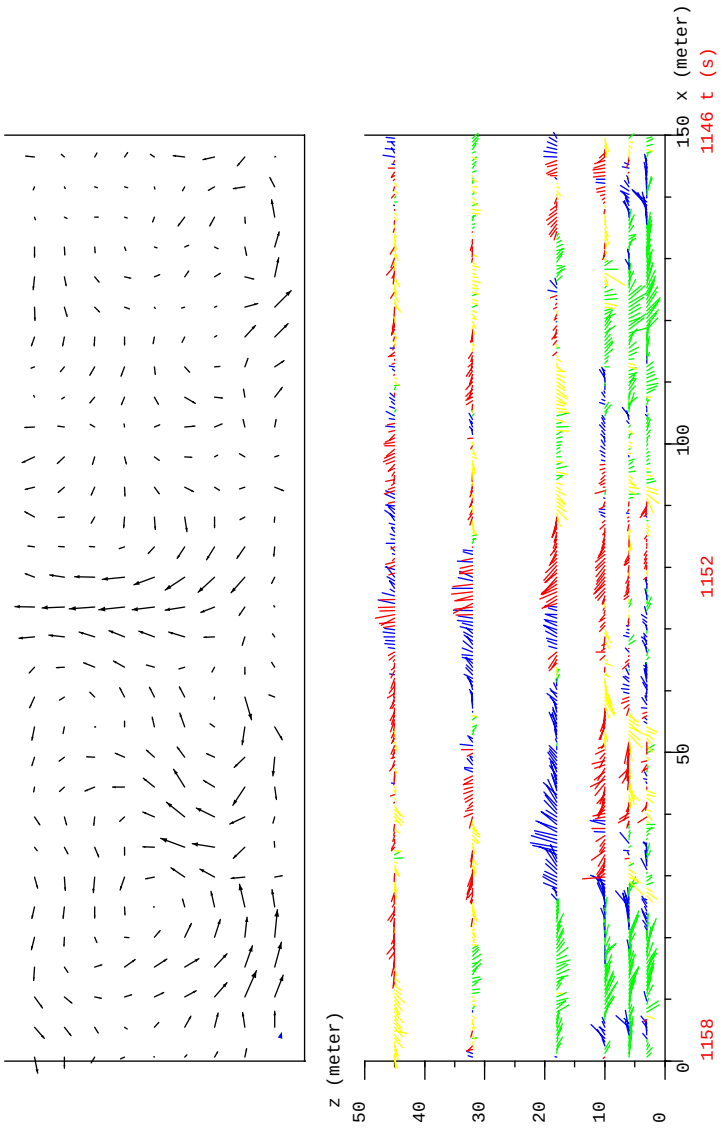

Figure 3.9: Plume Flow.

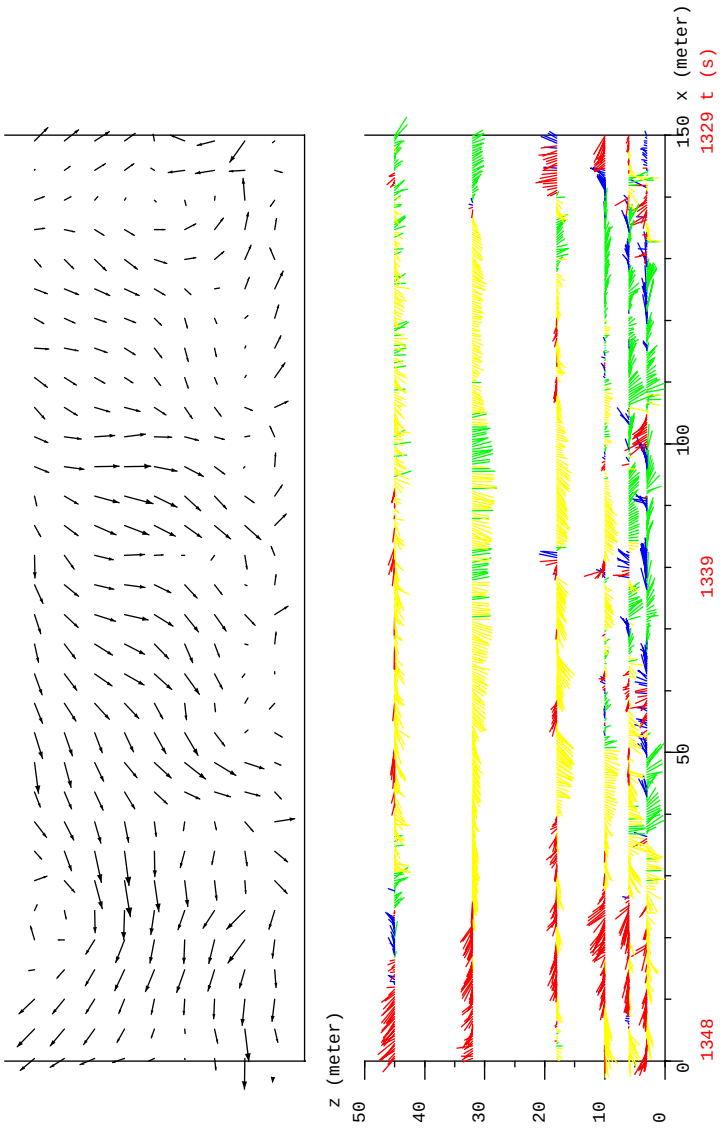

Figure 3.10: Downdraft Flow.

3.3 Characteristics of the Coherent Structures in the Near Neutral Marine Atmospheric Surface Layer

According to the temperature difference, or lapse rate, along the vertical direction to the wall, the atmospheric stability can be put into three kinds: stable, neutral and unstable ($\frac{\partial T}{\partial z} > 0$, $\frac{\partial T}{\partial z} = 0$ and $\frac{\partial T}{\partial z} < 0$). It is generally believed that the vertical motions are enhanced in a unstable atmosphere whereas they are damped in a stable atmosphere. The variation of lapse rate in the marine atmospheric surface layer is not as large as that in land atmospheric surface layer. Because of the large heat capacity of water, the radiative heat from the sun received by the oceans raises the water temperature only a little. So the stability of the marine atmospheric surface layer is typically nearer neutral than that of land atmospheric surface layer. For the investigation related to the coherent structures, a total of 24 data files (12 hours data) which were recorded in near neutral condition and with mean wind speed U_m = 5–12.6 m/s have been chosen from the RASEX data files.

In this section, the spatial and temporal characteristics of the coherent structures will be analyzed with the observation and statistics on the selected data files. The spatial and temporal characteristics of the coherent structures has been found to be related to the mean wind speed and temperature difference between higher level and sea surface. The effect of the mean wind speed and temperature difference on the spatial and temporal characteristics of the coherent structures will be discussed in Chapter 4. Since, as will be discussed in section 4.1, the mean wind speed is the main factor in affecting the spatial and temporal characteristics of the coherent structures and as will be discussed in section 4.2, the effect of the temperature difference on the coherent structures is not as evident as that of the mean wind speed in the near neutral marine atmospheric surface layer. Hence, for the sake of simplicity, only the mean wind speed is considered in the first step of the analysis. The selected data files have been divided into two groups only according to the

value of the mean wind speeds, higher or lower wind speed. The mean wind speed range of lower wind speed group is U_m = 5.0–8.0 m/s, the higher wind speed one is U_m = 8.1–12.6 m/s.

The profiles of normalized friction velocity ($\sqrt{-\overline{u'w'}}/U_{10}$, where U_{10} is mean wind speed at 10 m height above sea level) over the marine atmospheric surface layer are shown in Figures 3.11 and 3.12, which are based on the examined data files. The normalized friction velocity is on the order of 0.02–0.04 at mean wind speed of U_{10} = 5.0–8.0 m/s, whereas it is on the order of 0.03–0.05 at mean wind speed of U_{10} = 8.1–12.6 m/s. The kinematic Reynolds stress ($-\overline{u'w'}$) in the marine atmospheric surface layer is on the order of 0.1 m^2/s^2. The general variation tendency of the normalized friction velocity with the height and mean wind speed is shown in Figure 3.13, which is obtained by averaging the normalized friction velocities in two wind speed groups respectively. As shown in Figure 3.13, the average of the normalized friction velocity increases with the increase of the mean wind speed in the marine atmospheric surface layer.

The streamwise spatial length distributions of the ejection and sweep motions are shown in Figures 3.14 to 3.21. Only those ejection and sweep events which extend from the wall to the height of 45 m have been included in these figures. If the streamwise length of these events is less than 10 m, they often can not extend the height of 45 m. Hence the streamwise spatial length of the ejection and sweep events is greater than 10 m in these figures. The range of the streamwise spatial length of the ejection and sweep events is from 20 m to 250 m which may depend on the life stage of the ejection and sweep events passing the probe and other ambient conditions. The shorter events may be at the initial stage, the medium events at the developing stage while the longer events at the fully developed stage.

The streamwise length of individual ejections, which are observed to occur alone and sep-

arate from other coherent motions in the marine atmospheric surface layer, is seen to be 20–130 m at mean wind speed of 5.0–8.0 m/s as shown in Figure 3.14 and 30–150 m at mean wind speed of 8.1–12.6 m/s as shown in Figure 3.15. The streamwise length of ejections in shear layer events, which form a shear layer with the immediate upstream sweeps in the marine atmospheric surface layer, is 20–190 m at mean wind speed of 5.0–8.0 m/s as shown in Figure 3.16 and 20–210 m at mean wind speed of 8.1–12.6 m/s as shown in Figure 3.17. The streamwise length of individual sweeps, which occur alone and separate from other coherent motions, is 20–180 m at mean wind speed of 5.0–8.0 m/s as shown in Figure 3.18 and 20–200 m at mean wind speed of 8.1–12.6 m/s as shown in Figure 3.19. The streamwise length of sweeps in shear layer events, which form a shear layer with the immediate downstream ejections, is 30–220 m at mean wind speed of 5.0–8.0 m/s as shown in Figure 3.20 and 20–250 m at mean wind speed of 8.1–12.6 m/s as shown in Figure 3.21. Comparing the figures of length distribution, a conclusion can be made that the maximum streamwise length of the individual sweeps is longer than that of the individual ejections at the same range of mean wind speed and the maximum streamwise length of the sweeps in shear layer events is also longer than that of the ejections in shear layer events at the same range of mean wind speed. The maximum streamwise length of the events may be the streamwise length of the fully developed events. Based on the figures of length distribution of the ejection and sweep motions, it is clear that the streamwise spatial length of the fully developed ejection and sweep events increases as the mean wind speed increases.

After examining the selected data files, statistics of the temporal characteristics of the coherent structures in the marine atmospheric surface layer have been listed in Tables 3.1 and 3.2. In the tables the frequency of occurrence of the coherent motions is given for each 30 minute data file. The mean frequency of the ejections and sweeps is 6.5×10^{-3} s^{-1} and 6.3×10^{-3} s^{-1} respectively, and the duration of the ejections and sweeps approximates 3–36 s at mean wind speed of 5.0–8.0 m/s. The mean frequency of the ejections and sweeps is

1.2×10^{-2} s^{-1} and 1.4×10^{-2} s^{-1} respectively, and the duration of the ejections and sweeps approximates 2–27 s at mean wind speed of 8.1–12.6 m/s. Heathershaw (1974) reported that the frequency and duration of the ejections and sweeps are of the order of 10^{-2} s^{-1} and 5–10 s respectively in bottom boundary layer of the sea tidal currents. Gordon (1975) found that the mean period and duration of the ejections and sweeps are approximately 70 s and 9 s respectively in a tidal boundary layer. The frequency of the ejections and sweeps in the marine atmospheric surface layer is relatively smaller but their duration is longer as compared with those in low Reynolds number turbulent boundary layer flow.

From the figures of length distribution one more conclusion can be reached that the maximum streamwise spatial length of the ejections and sweeps in shear layer events is greater than that of the individual ejection and sweep events at the same range of mean wind speed. The inclined angle of the shear layer is observed to vary from 30° to 70°. The longer the shear layer is, the smaller the inclined angle. The longer shear layer may well extend above the maximum measuring height to a much higher level and form a much larger scale motion. Based on Tables 3.1 and 3.2, the mean frequency of the shear layer is about 3.8×10^{-3} s^{-1} at the mean wind speed of 5.0–8.0 m/s, while it is about 6.7×10^{-3} s^{-1} at the mean wind speed of 8.1–12.6 m/s.

Because of the limitation of the maximum measuring height and measuring space between the sensors in the experiment data, those transverse vortices whose diameter is greater than 40 m or less than 10 m can not be traced in the present work. In the current measuring range the transverse vortices are seen to exist in every region from the wall to the maximum measuring height and their diameters are from 10 m to 40 m. They may exist in every region of the overall marine atmospheric surface layer and may indeed be the principal elements in turbulence production. As indicated in Tables 3.1 and 3.2, the mean frequency of the transverse vortices approximates to 7.0×10^{-3} s^{-1} at the mean wind speed of 5.0–8.0 m/s, while it approximates to 9.7×10^{-3} s^{-1} at the mean wind speed of 8.1–12.6 m/s.

Some times a combination event of the shear layer and transverse vortex, or the shear layer back of large transverse vortex, can be seen in the marine atmospheric surface layer. In this combination event of the shear layer and the large transverse vortex, the streamwise extent of the shear layer is generally longer (100–350 m), the diameter of the transverse vortex is larger (20–40 m) and its center is located at a higher vertical position (above 25 m in height). From Tables 3.1 and 3.2, the mean frequency of this event is about 1.3×10^{-3} s^{-1} at the mean wind speed of 5.0–8.0 m/s and it is about 1.6×10^{-3} s^{-1} at the mean wind speed of 8.1–12.6 m/s. If more probes are put at much higher levels than the height of 45 m, more shear layer back motions and much larger transverse vortices may be seen in the marine atmospheric surface layer.

When the air temperature at higher level is lower than that at sea level in the marine atmospheric surface layer, the plume and downdraft motions can be observed. The streamwise spatial length of the plume and downdraft motions is generally from 20 m to 50 m in the present data. As compared with the streamwise spatial length of the other coherent motions the streamwise spatial length of the plume and downdraft motions is generally not very long, since the plume and downdraft motions mainly depend on the temperature difference which is not very large in the near neutral marine atmospheric surface layer. In addition, the mean wind speed at lower level of the surface layer may be lower than the real convective speed of the plume and downdraft motions. The frequency of the plumes and downdraft is of order of 10^{-3} s^{-1}, which varies with both the temperature difference and the mean wind speed.

These figures of length distribution as well as the tables of frequency of occurrence of the coherent structures give a general conception of the spatial and temporal characteristics of the coherent structures in the marine atmospheric surface layer. It is obvious that the ejection, sweep and shear layer "back" of large transverse vortex events observed in the marine atmospheric surface layer are qualitatively similar to those observed in lower

Reynolds number turbulent boundary layer flow. Hence a strong argument can be made that these events are universal phenomena in turbulent boundary layer. The nature of these events both in the marine atmospheric surface layer and in lower Reynolds number turbulent boundary layer flow appears to be the same while their spatial and temporal scales are not the same. The streamwise spatial length of those events in the marine atmospheric surface layer is generally longer (20–250 m for ejections and sweeps), their frequency is smaller ($10^{-2} - 10^{-3}$ s^{-1} for ejections and sweeps), and their duration is longer (2–36 s for ejections and sweeps).

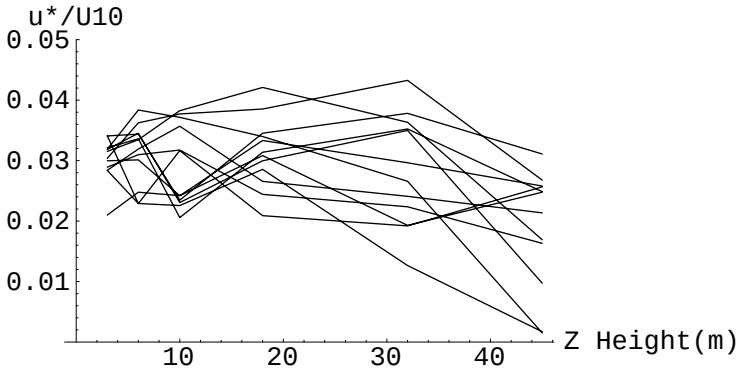

Figure 3.11: Profiles of normalized friction velocity (u_*/U_{10}) over the marine atmospheric surface layer, U_{10} =5.0–8.0 m/s, where U_{10} is mean wind speed at 10 m height above sea level.

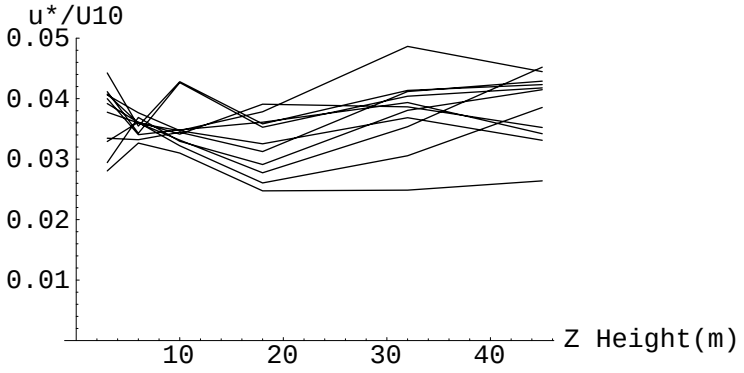

Figure 3.12: Profiles of normalized friction velocity (u_*/U_{10}) over the marine atmospheric surface layer, U_{10} =8.1–12.6 m/s, where U_{10} is mean wind speed at 10 m height above sea level.

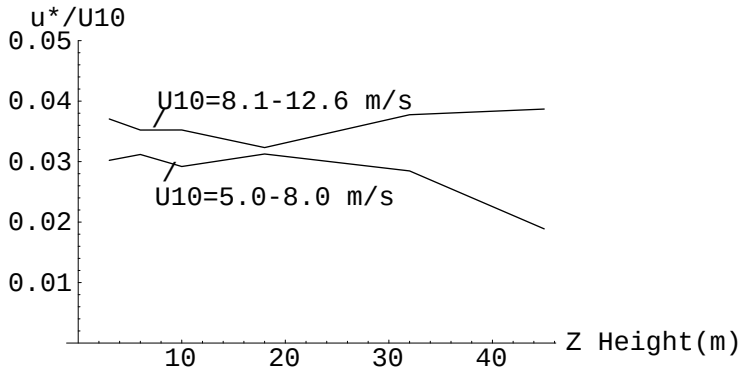

Figure 3.13: Average of normalized friction velocity (u_*/U_{10}) profiles over the marine atmospheric surface layer.

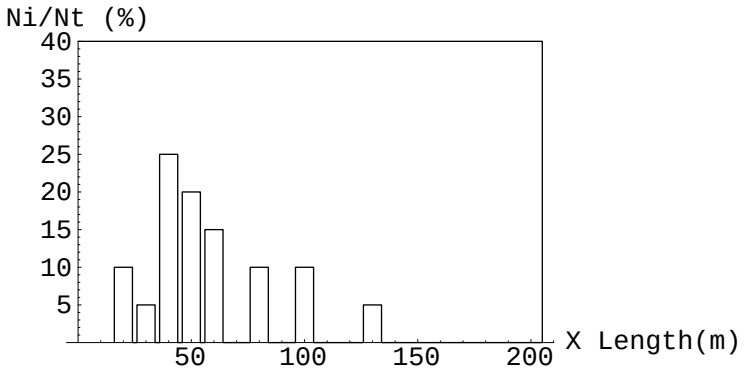

Figure 3.14: Length distribution of individual ejections, $U_m = 5.0$–8.0 m/s.

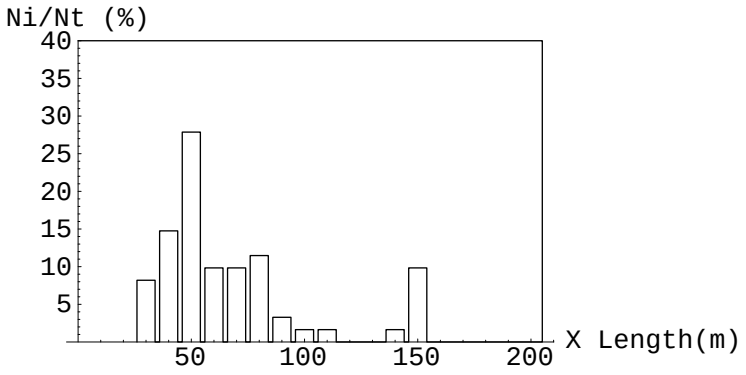

Figure 3.15: Length distribution of individual ejections, $U_m = 8.1$–12.6 m/s.

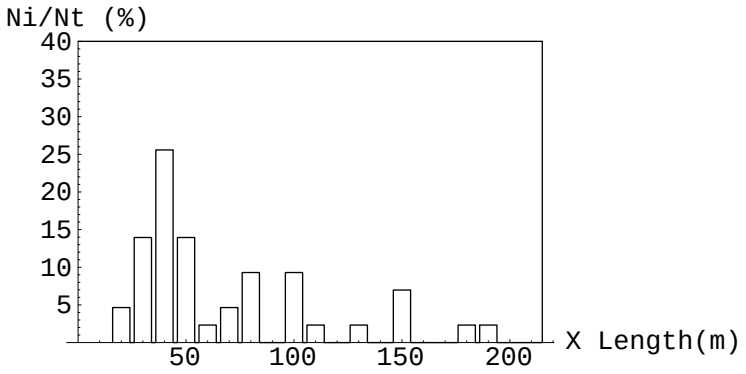

Figure 3.16: Length distribution of ejections in shear layer, $U_m = 5.0$–8.0 m/s.

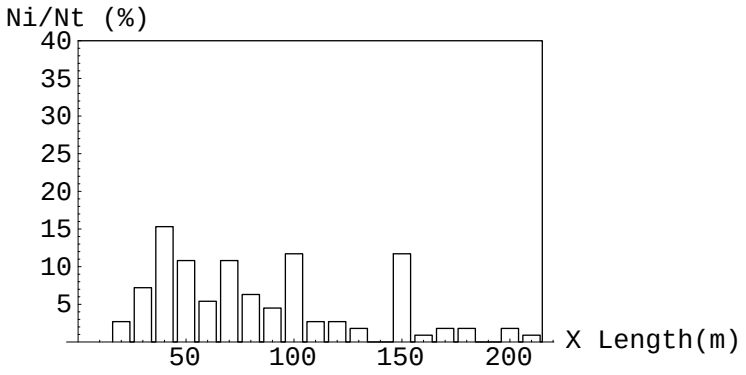

Figure 3.17: Length distribution of ejections in shear layer, $U_m = 8.1$–12.6 m/s.

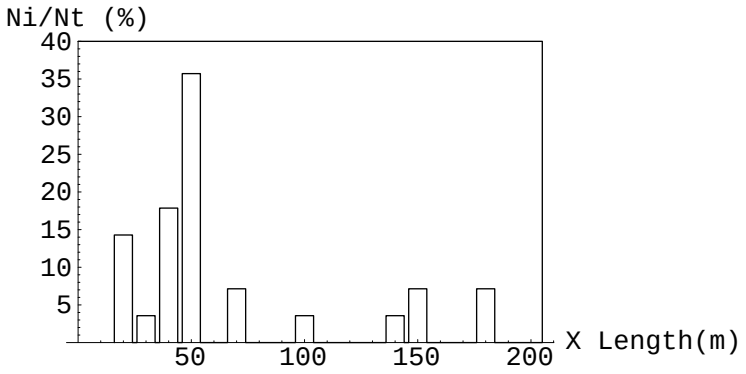

Figure 3.18: Length distribution of individual sweeps, $U_m = 5.0$–8.0 m/s.

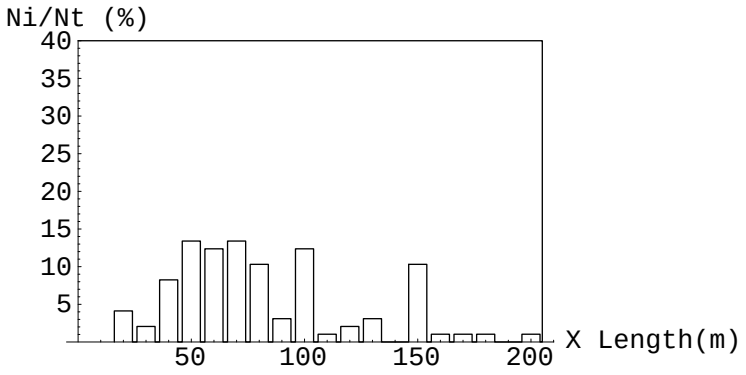

Figure 3.19: Length distribution of individual sweeps, $U_m = 8.1$–12.6 m/s.

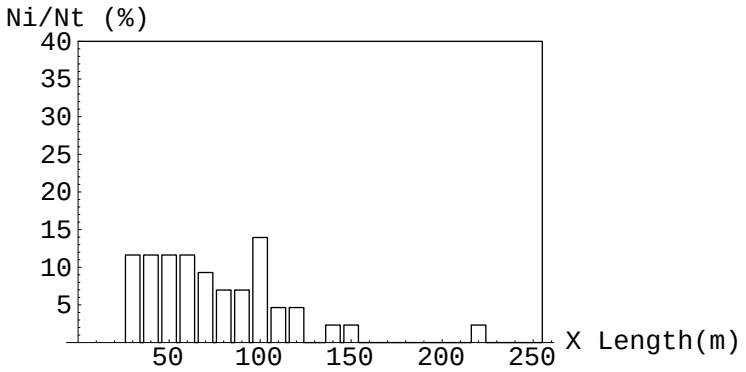

Figure 3.20: Length distribution of sweeps in shear layer, $U_m = 5.0$–8.0 m/s.

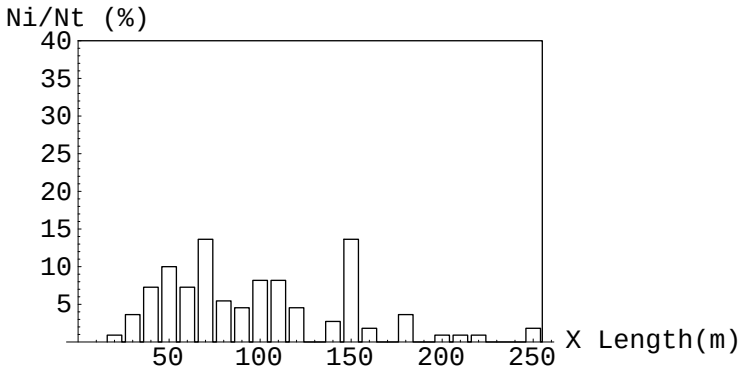

Figure 3.21: Length distribution of sweeps in shear layer, $U_m = 8.1$–12.6 m/s.

Table 3.1: Frequency of the coherent motions (30 minutes for each file), U_m = 5.0–8.0 m/s.

File	U_m (m/s)	dT47-10 (°C)	Q_2	Q_4	SL	TV	CS	P	D
140316	5.02	-0.409	3	4	1	7	2	11	13
151552	5.42	-0.156	2	2	3	5	2	6	7
021337	5.53	-0.403	3	2	6	5	3	6	3
131416	5.95	-0.123	2	3	0	15	2	0	1
132346	6.04	-0.392	3	3	5	13	3	22	15
021307	6.28	-0.431	5	3	3	12	4	12	6
131346	6.40	-0.156	9	4	3	14	1	3	3
140416	6.52	-0.427	8	7	3	13	2	11	9
131216	6.60	-0.194	4	5	3	11	5	1	1
131246	6.84	-0.191	8	7	4	7	1	3	0
131316	6.90	-0.179	7	3	4	14	0	10	6
281542	7.85	0.284	4	7	12	7	1	0	0
281412	7.90	0.343	1	4	9	14	1	0	0
160546	8.00	-0.521	10	11	7	8	5	15	14

Note: The shorthand notation of the tables is listed at next page.

dT47–10: Temperature difference between a height of 47 m and 10 m above sea surface;
Q_2: The second quadrant events (x-z plane), or ejection events;
Q_4: The fourth quadrant events (x-z plane), or sweep events;
SL: Shear layer events;
TV: Transverse vortex events;
CS: Combination structure events of shear layer and transverse vortex;
P: Plume events;
D: Downdraft events.

Table 3.2: Frequency of the coherent motions (30 minutes for each file), $U_m = 8.1$–12.6 m/s.

File	U_m (m/s)	dT47-10 (°C)	Q_2	Q_4	SL	TV	CS	P	D
040037	8.12	-0.252	9	14	9	16	6	8	5
281442	8.39	0.089	5	7	15	6	1	0	0
040007	8.39	-0.317	8	9	1	20	3	16	8
152046	8.88	-0.414	5	12	12	5	4	12	10
011105	9.18	-0.432	9	16	13	8	1	13	3
041353	10.76	-0.121	10	12	2	16	1	2	5
041323	11.21	-0.028	12	10	4	16	0	0	7
010152	11.94	-0.486	11	21	15	20	5	8	2
010022	12.16	-0.504	11	9	4	18	4	13	7
010122	12.58	-0.503	16	19	17	22	3	8	3

Chapter 4

THE COHERENT STRUCTURES AND AMBIENT CONDITIONS

4.1 Relationship Between the Coherent Structures and Mean Wind Speeds

It has been observed in the present work that the mean wind speed plays a leading role in affecting the spatial and temporal characteristics of the coherent structures in the near neutral marine atmospheric surface layer. It has been noted, as mentioned previously, that as the mean wind speed increases, the maximum spatial length of the ejections and sweeps increases. There is also a very evident tendency for the occurrence frequency of the ejection and sweep motions to increase as the mean wind speed increases, as shown in Figures 4.1 and 4.2. Therefore, with the increase of the mean wind speed it is expected to see more of and longer ejection and sweep motions in the marine atmospheric surface layer.

The statistics indicate that the mean frequency of the ejections is greater than that of sweeps at the mean wind speed of 5.0–8.0 m/s, while the mean frequency of the ejections is less than that of sweeps at the mean wind speed of 8.1–12.6 m/s. This means that the outer region may become more active in turbulence production as the mean wind speed increases which leads to more of high speed entrainment motions in the marine atmospheric surface layer.

In the region below the maximum probe height, it has been seen that the maximum spatial length of the shear layers increases with the increase of the mean wind speed. At higher mean wind speed ($U_m > 6.0$ m/s), two or more typical larger shear layer vortices along with some longer shear layer can be observed. These longer shear layers often are of small inclined angles to the wall. The frequency of occurrence of the shear layers seems to increase as the mean wind speed increases as shown in Figure 4.3, although the tendency of the increase is not very obvious.

It has not been seen in the present data that the spatial size and location of the transverse vortices have apparent relation to the mean wind speed. However, with the increase of the mean wind speed, there exists a few traces of large diameter transverse vortices whose center may well overpass the maximum height of the probe and only a small part of which can be seen in the present probe region. Hence the spatial size of the transverse vortices may increase with the increase of the mean wind speed in the overall marine atmospheric surface layer. On the other side, with the decrease of the mean wind speed there may exist more of the smaller transverse vortices which can not be traced because their diameter is less than the large space between the sensors. Anyway, it has been found that the frequency of occurrence of the transverse vortices, which can be traced in the present work, tends to increase as the mean wind speed increases as shown in Figure 4.4. The increase of the transverse vortices may cause more of ejections, sweeps and shear layers. Thus an argument can well be made that as the mean wind speed increases, the turbulent strength will also

increase.

The wind speed has no evident effect on the frequency of the combination structures of the shear layers and the large transverse vortices in the present data, as shown in Figure 4.5. However, as the mean wind speed increases there may exist more of much larger shear layers and transverse vortices, which can not be seen due to the limitation of the maximum height of the probe. Therefore the frequency of the shear layer back of the large transverse vortex may increase as the mean wind speed increases in the overall marine atmospheric surface layer.

The spatial size of the plume and downdraft motions has not been found to vary obviously with the variation of the mean wind speed, while their occurrence frequency will decrease with the increase of the mean wind speed at constant temperature difference. The increase of the mean wind speed will generally suppress the occurrence of the plume and downdraft motions which are caused by the variation of the air buoyancy. More of the data files have to be examined in order to further analyze the relationship between the plume and downdraft motions and the mean wind speed.

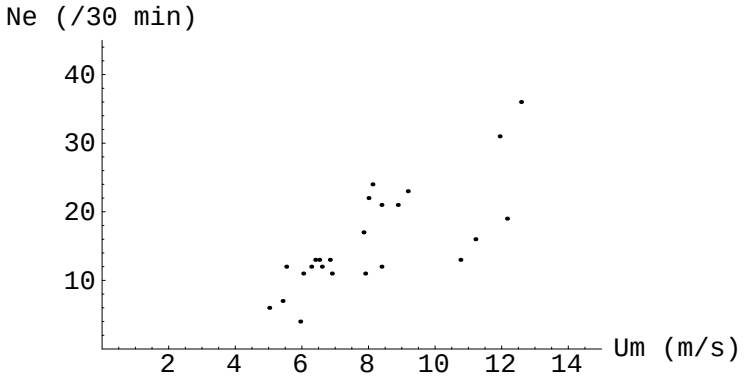

Figure 4.1: Frequency of ejections at different mean wind speeds.

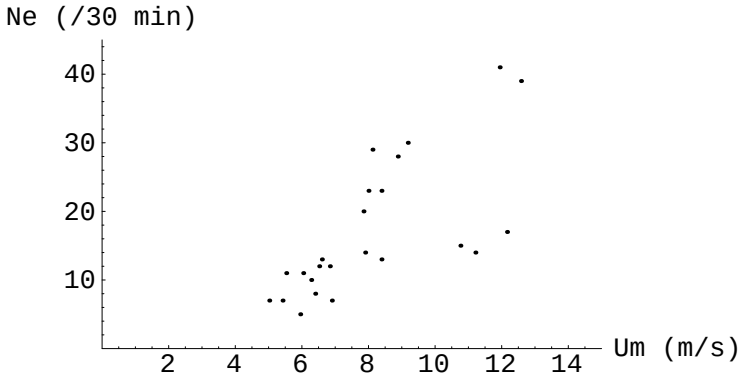

Figure 4.2: Frequency of sweeps at different mean wind speeds.

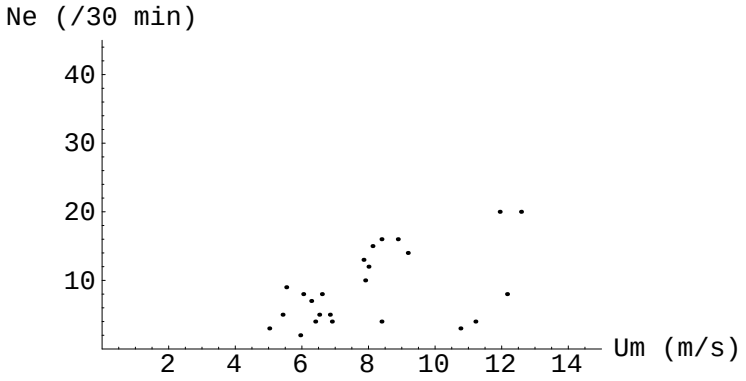

Figure 4.3: Frequency of shear layers at different mean wind speeds.

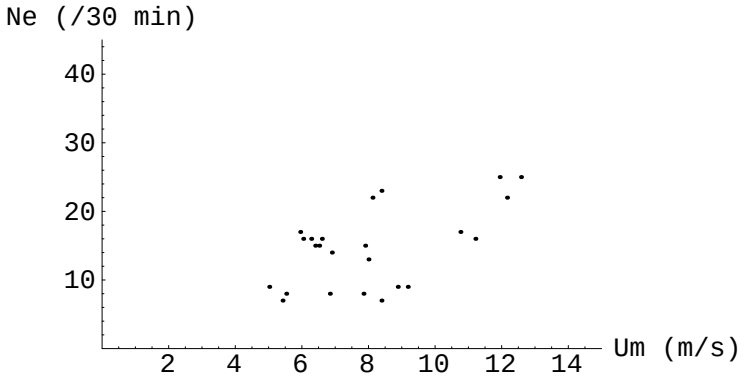

Figure 4.4: Frequency of transverse vortices at different mean wind speeds.

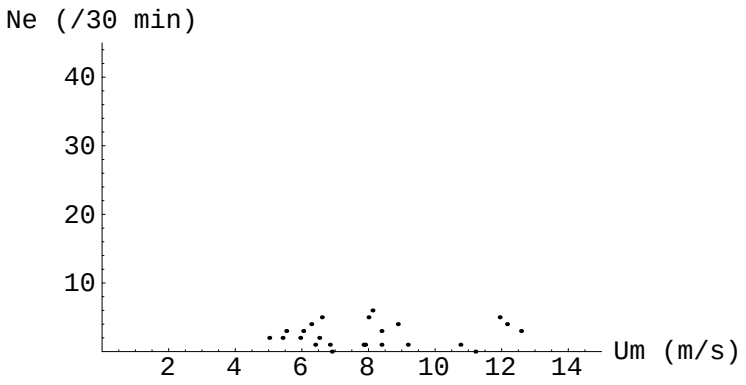

Figure 4.5: Frequency of combination structures of shear layers and transverse vortices at different mean wind speeds.

4.2 Relationship Between the Coherent Structures and Temperature Differences

As previously mentioned, the stability of the marine atmospheric surface layer is generally near neutral and it is generally believed that the vertical motions are enhanced in a unstable atmosphere whereas they are damped in a stable atmosphere. For the near neutral marine atmospheric surface layer there seems no very evident relationship between the spatial size of the coherent motions and the temperature gradient, while it has been seen that the fluctuation components of the wind velocity usually decrease as the vertical temperature gradient becomes positive under the same wind speed condition. As the marine atmospheric surface layer becomes more stable, the height to which the coherent motions can extend seems to decrease.

The frequency of the coherent motions generally decreases as the increase of the temperature at higher level (47 m above sea surface), as shown from Figures 4.6 to 4.11. It has been observed that the occurrence of the plume and downdraft motions mainly depends on the temperature differences. The frequency of plume and downdraft motions tends to decrease as the increase of the temperature at higher level, as shown in Figures 4.6 and 4.7. When the marine atmospheric surface layer becomes stable there is no plume and downdraft motions in the marine atmospheric surface layer.

As shown in Figures 4.8 and 4.9, the frequency of ejection and sweep motions will decrease with the decrease of the temperature differences. With the stability of the marine atmospheric surface layer becomes unstable, the more ejection and sweep events will be seen. Although the effect of temperature differences on the occurrence of the shear layers and transverse vortices is not as evident as on that of the plumes, the frequency of these two coherent motions seems to decrease with the decrease of the temperature differences, as

shown in Figures 4.10 and 4.11. In the present observing region there seems little relationship between the temperature differences and the frequency of the combination structures of the shear layers and transverse vortices, as shown in Figure 4.12. However, as the temperature differences increase greatly, or marine atmospheric surface layer becomes unstable, the spatial size of some transverse vortices will increase larger and the center of these larger transverse vortices may be located at a height above the present observing height. Therefore, the frequency of the combination structures as well as the transverse vortices may increase with the increase of the temperature differences in overall marine atmospheric surface layer. In general, the effect of temperature differences on the occurrence of the buoyancy related plume and downdraft motions is more evident than on that of the other shear related coherent motions in the marine atmospheric surface layer.

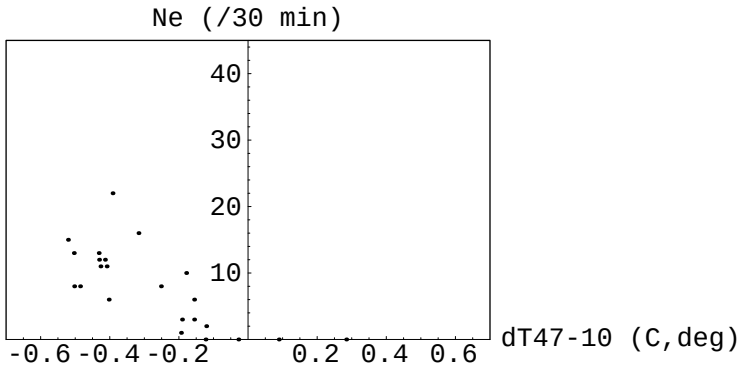

Figure 4.6: Frequency of plumes at different temperature differences between 47 m and 10 m heights above sea surface.

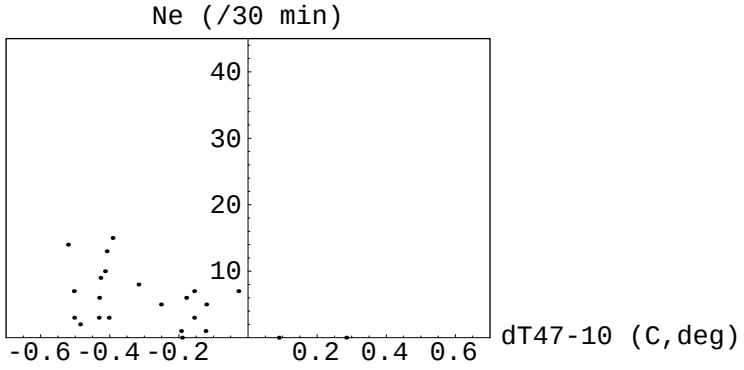

Figure 4.7: Frequency of downdrafts at different temperature differences between 47 m and 10 m heights above sea surface.

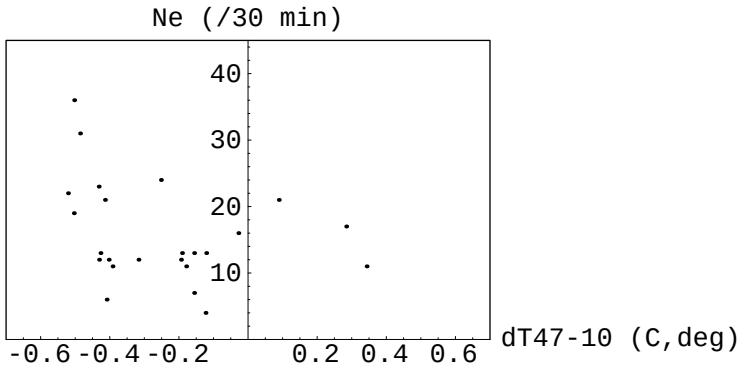

Figure 4.8: Frequency of ejections at different temperature differences between 47 m and 10 m heights above sea surface.

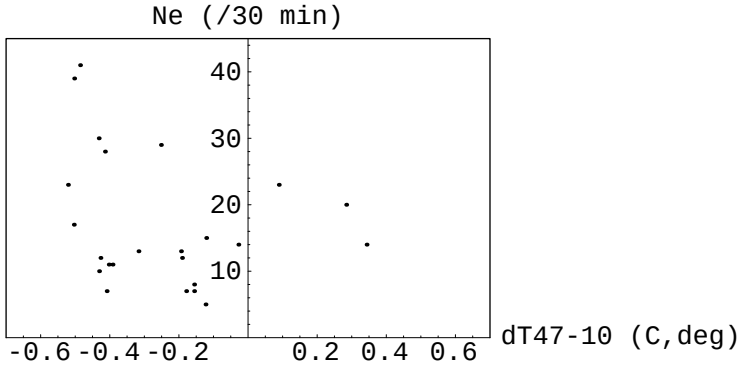

Figure 4.9: Frequency of sweeps at different temperature differences between 47 m and 10 m heights above sea surface.

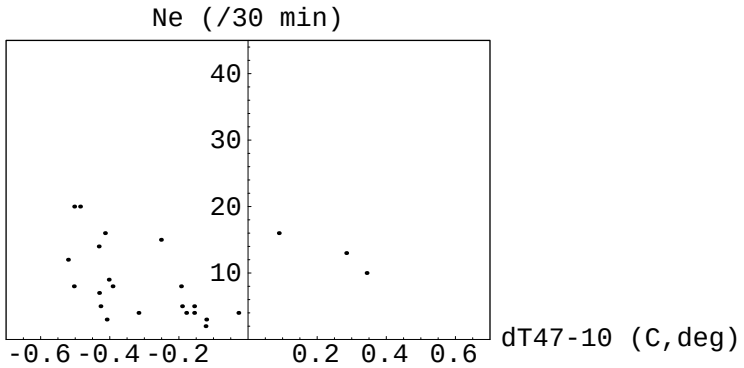

Figure 4.10: Frequency of shear layers at different temperature differences between 47 m and 10 m heights above sea surface.

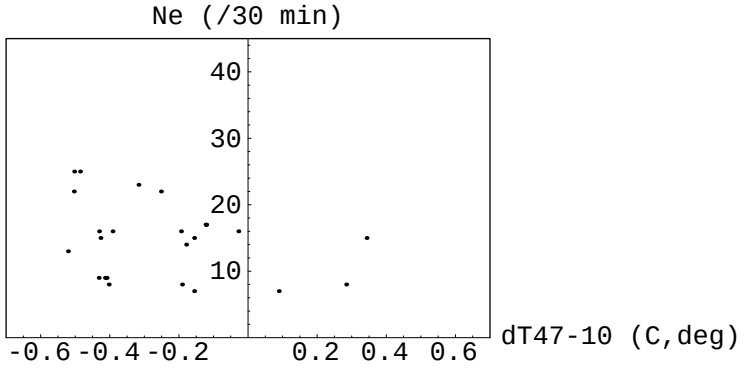

Figure 4.11: Frequency of transverse vortices at different temperature differences between 47 m and 10 m heights above sea surface.

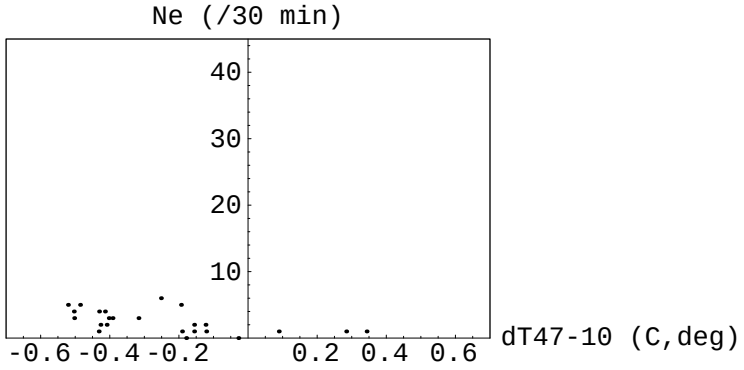

Figure 4.12: Frequency of combination structures of the shear layers and transverse vortices at different temperature differences between 47 m and 10 m heights above sea surface.

Chapter 5

DISCUSSION AND CONCLUSIONS

With the time-series of wind velocity components at multi-points, various coherent motions have been identified and counted. The signature, size and frequency of these coherent motions have been studied. From above work it is clear that some of the coherent motions observed in the marine atmospheric surface layer are very similar to those seen in the laboratory turbulent boundary layer. The events of ejection, sweep, transverse vortex and shear layer back of large transverse vortex in the marine atmospheric surface layer are the same coherent events classified by Robinson (1991), while the events of plume and downdraft are the coherent motions which exist only in the atmospheric boundary layer. Hence the coherent events of the ejection, sweep, transverse vortex and shear layer back of large transverse vortex could be universal in turbulent boundary layer.

The spatial and temporal characteristics of these coherent structures have been studied quantitatively. The ejection events which lift low momentum air from the surface to a height of 45 m have been counted. It is found that the streamwise spatial length of the ejections is 20–190 m at mean wind speed of 5.0–8.0 m/s and 20–210 m at mean wind

speed of 8.1–12.6 m/s. The streamwise spatial length of the sweeps is 20–220 m at mean wind speed of 5.0–8.0 m/s and 20–250 m at mean wind speed of 8.1–12.6 m/s. The mean frequency of the ejections and sweeps is 6.5×10^{-3} s^{-1} and 6.3×10^{-3} s^{-1} respectively, and the duration of the ejections and sweeps approximates 3–36 s at mean wind speed of 5.0–8.0 m/s. The mean frequency of the ejections and sweeps is 1.2×10^{-2} s^{-1} and 1.4×10^{-2} s^{-1} respectively, and the duration of the ejections and sweeps approximates 2–27 s at mean wind speed of 8.1–12.6 m/s. The maximum spatial length of the sweeps is longer than that of the ejections. The variation of the spatial length of ejections and sweeps may indicate the state of development of these two events.

One point needed to be discussed here is time scaling. This has been a controversial point as there are inner and outer time scaling respectively. The inner time scaling is $T = \nu/u_*^2$, in which $u_*^2 = \tau_0/\rho$, while the outer time scaling is $T = \delta/U_\infty$. In the present work, ν is of order of 10^{-5} m^2/s, u_* is order of 10^{-1} m/s, U_∞ is of order of 10 m/s and the thickness of the marine atmospheric boundary layer extends up to 1 km or more in height which leads the inner and outer time scaling to be order of 10^{-3} s and 10^2 s respectively. The outer time scaling agrees with the mean period of the ejections and sweeps being of order of 10–10^2 s found in the present work, while the inner time scaling is obviously not suitable for the ejection and sweep events in the marine atmospheric surface layer. Therefore the outer time scaling is more suitable for the ejection and sweep events in the marine atmospheric surface layer.

When sweeps follow downstream ejections, an inclined shear layer is formed between the upstream sweeps and downstream ejections and some transverse vortices can often be seen on longer shear layers. These shear layer transverse vortices may be created by the roll up of the shear layer. It has been observed that the inclined angle of the shear layer varies from 30° to 70° with the height and length of the the shear layer. The lower in height and longer in length, the smaller the inclined angle. The mean frequency of occurrence of the

shear layers is about 3.8×10^{-3} s^{-1} at the mean wind speed of 5.0–8.0 m/s and 6.7×10^{-3} s^{-1} at the mean wind speed of 8.1–12.6 m/s.

With the velocity components at multi-heights the transverse vortices have been traced. In the present work it has been seen that the transverse vortices exist in every region from the wall to the maximum probe height and their diameter is up to 40 m. The mean frequency of occurrence of the transverse vortices is of order of 10^{-3} s^{-1} at the mean wind speed of 5.0–12.6 m/s. There may exist much larger transverse vortices over the region above the maximum height of the present probe because only a small part of these larger transverse vortices may be seen by the present probe. It has been observed that some large transverse vortices indeed cause the ejection and sweep motions. Immediately after a large transverse vortex past, an inclined shear layer was formed between the low speed fluid (or ejections) trailing the large transverse vortex and the following high speed fluid (or sweeps). Therefore the transverse vortices could be the principal elements in turbulence production.

When the air temperature at higher level is lower than that at sea level in the marine atmospheric surface layer, the plume and downdraft motions can be observed. The streamwise spatial length of the plume and downdraft motions is generally from 20 m to 50 m and the mean frequency of occurrence of the plume and downdraft motions is of order of 10^{-3} s^{-1}. Although the mean frequency of occurrence of the plume and downdraft motions is the same order as that of the other shear related coherent motions, the streamwise spatial extent of the plume and downdraft motions is generally less than that of the ejection and sweep motions. Hence, one argument can be made that in the near neutral marine atmospheric surface layer the shear related coherent motions are dominant motions in turbulence production.

Analysis indicates that the wind speed is a dominant factor in affecting the spatial and temporal characteristics of the coherent structures in the marine atmospheric surface layer.

It is observed that both the maximum streamwise length and mean frequency of the ejections, sweeps and shear layers increase with the increase of the mean wind speed which leads the turbulence strength to increase. The frequency of the transverse vortices also increases with the mean wind speed, although their size and location have little relation to the mean wind speed in the depth of the present probe. The increase of the mean wind speed will generally damp the occurrence of the plume and downdraft motions.

The temperature difference between higher level and sea surface is the second main factor affecting the spatial and temporal characteristics of the coherent structures in the marine atmospheric surface layer. It has been noted that the strength and frequency of the coherent motions usually decrease as the vertical temperature gradient becomes positive under constant wind speed. As the marine atmospheric surface layer becomes more stable the coherent motions will be suppressed. The effect of the temperature difference on the coherent motions is not as evident as that of the mean wind speed. However, the effect of the temperature difference on the buoyancy related plume and downdraft motions is more evident than on the other shear related coherent motions in the marine atmospheric surface layer.

As mentioned previously, in the present work the observation of the coherent motions has been limited in a height of 45 m above sea surface and the measurement of the wind velocity is only in one plane. For further description of spatial and temporal characteristics of the shear layer back of transverse vortex, the motions at higher level (higher than 45 m above sea level) need to be studied because of much larger scale of this type of coherent motion. A great deal work also needs to be done before a clear three-dimensional picture of these coherent motions in the marine atmospheric surface layer can be drawn because of the three-dimensional characteristics of these coherent structures.

Bibliography

[1] Azad, R. S., *The Atmospheric Boundary Layer for Engineers*, Kluwer Academic Publishers, Boston, 1993.

[2] Barthelmie, R. J., M. S. Courtney, J. Høstrup and P. Sanderhoff, The Vindeby Project: A Description. **RISØ-R-741(EN)**, Risø National Laboratory, Roskilde, Denmark, March 1994.

[3] Blackwelder, R. F. and R. E. Kaplan, On the Bursting Phenomenon Near the Wall in Bounded Shear Flows, *J. Fluid Mech., 76,* 89–112, 1976.

[4] Bogard, D. G. and W. G. Tiederman, Burst Detection With Single Point Velocity Measurements, *J. Fluid Mech., 162,* 389–413, 1986.

[5] Boppe, R. S. and W. L. Neu, Quasi-Coherent Structures in the Marine Atmospheric Surface Layer, *J. Geo. Res., 100(C10),* 1995.

[6] Boppe, R. S., Structure of Turbulence in the Marine Atmospheric Surface Layer, Ph.D. Dissertation, Virginia Polytechnic Institute and State University, Blacksburg, 1995.

[7] Corino, E. R. and R. S. Brodkey, A Visual Investigation of the Wall Region in Turbulent Flow, *J. Fluid Mech., 37,* 1–30, 1969.

[8] Garratt, J. R., *The Atmospheric Boundary Layer,* Cambridge University Press, Cambridge 1992.

[9] Gordon, J. R., Intermittent Momentum Transport in a Geophysical Boundary Layer, *Nature, 248,* 392–394, 1974.

[10] Gordon, M. C., Period Between Bursts at High Reynolds Number, *Phys. Fluids, 18(2),* 141–143, 1975.

[11] Heathershaw, A. D., "Bursting" Phenomena in the Sea, *Nature, 248,* 394–395, 1974.

[12] Högström, U. and H. Bergström, Organized Turbulence Structures in the Near-Neutral Atmospheric Surface Layer, *Journal of the Atmospheric Sciences, 53, No.17,* 2452–2464, 1996.

[13] Kaimal, J. C. and J. J. Finnigan, *Atmospheric Boundary Layer Flow: Their Structure and measurement,* Oxford University Press, New York, 1994.

[14] Kim, H. T., S. J. Kline and W. C. Reynolds, Production of Turbulence Near a Smooth Wall in a Turbulent Boundary Layer, *J. Fluid Mech., 50,* 133–160, 1971.

[15] Kline, S. J., W. C. Reynolds, F. A. Schraub and P. W. Runstadler, The Structure of Turbulent Boundary Layer, *J. Fluid Mech., 30,* 741–773, 1967.

[16] Lu, S. and W. W. Willmarth, Measurements of the Structure of the Reynolds Stress in a Turbulent Boundary Layer, *J. Fluid Mech., 60,* 481–511, 1973.

[17] Panofsky, H. A. and J. A. Dutton, *Atmospheric Turbulence: Models and Methods for Engineering Applications,* John Wiley, New York, 1984.

[18] Phong-anant, D., R. A. Antonia, A. J. Chambers and S. Rajagopalan, Features of the Organized Motion in the Atmospheric Surface Layer, *J. Geophys. Res., 85(C1),* 424–432, 1980.

[19] Robinson, S. K., A Perspective on Coherent Structures and Conceptual Models for Turbulent Boundary Layer Physics, *AIAA 21st Fluid Dynamics, Plasma Dynamics and Lasers Conference,* 1990.

[20] Robinson, S. K., Coherent Motions in the Turbulent Boundary Layer, *Annu. Rev. Fluid Mech., 23,* 601–639, 1991.

[21] Stull, R. B., *An Introduction to Boundary Layer Meteorology*, Kluwer Academic Publishers, Boston, 1988.

[22] Tiederman, W. G., Eulerian Detection of Turbulent Bursts, *Near Wall Turbulence: 1988 Zoran Zarić Memorial Conference*, 874–887, Hemisphere Publishing Corporation, New York, 1988.

VITA

The author was born in Chongqing, China on May 10, 1958. He received his Bachelor of Science Degree in Naval Architecture from the Harbin Shipbuilding Engineering Institute, Harbin, China in January, 1982. Then he entered the Wuhan Ship Development and Design Institute, Wuhan, China. As a Naval Architect he designed a wide variety of high speed planing crafts and hydrofoil passenger ships for twelve years in the Wuhan Ship Development and Design Institute. In 1986–1987 he stayed in the Department of Aerospace and Ocean Engineering, Virginia Polytechnic Institute and State University, Blacksburg, USA as a visiting researcher. In August, 1995 he again entered the Department of Aerospace and Ocean Engineering, Virginia Polytechnic Institute and State University to pursue higher education.